AFWL-TR-76-70

AFWL-TR-
76-70

THE EFFECT OF INTENSE NUCLEAR RADIATION DAMAGE ON THE MECHANICAL PROPERTIES OF REENTRY VEHICLE-LIKE MATERIALS

Dr. Charles Stein

May 1976

Final Report

AIR FORCE WEAPONS LABORATORY
Air Force Systems Command
Kirtland Air Force Base, NM 87117

AFWL-TR-76-70

This final report was prepared for the Air Force Weapons Laboratory, Kirtland AFB, NM. Dr. Charles Stein (DYV) was the Laboratory Project Officer-in-Charge.

When US Government drawings, specifications, or other data are used for any purpose other than a definitely related Government procurement operation, the Government thereby incurs no responsibility nor any obligation whatsoever, and the fact that the Government may have formulated, furnished, or in any way supplied the said drawings, specifications, or other data is not to be regarded by implication or otherwise as in any manner licensing the holder or any other person or corporation or conveying any rights or permission to manufacture, use, or sell any patented invention that may in any way be related thereto.

This report has been reviewed by the Information Office (OI) and is releasable to the National Technical Information Service (NTIS). At NTIS, it will be available to the general public, including foreign nations.

This technical report has been reviewed and is approved for publication.

DR. CHARLES STEIN
Project Officer

FOR THE COMMANDER

C. D. STUBER
Major, USAF
Chief, Materials/Vulnerability
Hardening Branch

JOHN S. DEWITT
Lt Colonel, USAF
Chief, Technology Division

DO NOT RETURN THIS COPY. RETAIN OR DESTROY.

UNCLASSIFIED

SECURITY CLASSIFICATION OF THIS PAGE *(When Data Entered)*

REPORT DOCUMENTATION PAGE	READ INSTRUCTIONS BEFORE COMPLETING FORM
1. REPORT NUMBER (14) AFWL-TR-76-70 / 2. GOVT ACCESSION NO.	3. RECIPIENT'S CATALOG NUMBER
4. TITLE *(and Subtitle)* (6) THE EFFECT OF INTENSE NUCLEAR RADIATION DAMAGE ON THE MECHANICAL PROPERTIES OF REENTRY VEHICLE-LIKE MATERIALS.	5. TYPE OF REPORT & PERIOD COVERED (9) Final Report 6. PERFORMING ORG. REPORT NUMBER
7. AUTHOR(s) (10) ~~Dr.~~ Charles Stein	8. CONTRACT OR GRANT NUMBER(s) (16) AF-8809
9. PERFORMING ORGANIZATION NAME AND ADDRESS Air Force Weapons Laboratory (DYV) Kirtland AFB, NM 87117	10. PROGRAM ELEMENT, PROJECT, TASK AREA & WORK UNIT NUMBERS (17) 62601F; 88091502
11. CONTROLLING OFFICE NAME AND ADDRESS Air Force Weapons Laboratory (DYV) Kirtland AFB, NM 87117	12. REPORT DATE (11) May 1976 13. NUMBER OF PAGES 44
14. MONITORING AGENCY NAME & ADDRESS *(if different from Controlling Office)* (12) 47p.	15. SECURITY CLASS. *(of this report)* UNCLASSIFIED 15a. DECLASSIFICATION/DOWNGRADING SCHEDULE

16. DISTRIBUTION STATEMENT *(of this Report)*

Approved for public release; distribution unlimited.

17. DISTRIBUTION STATEMENT *(of the abstract entered in Block 20, if different from Report)*

18. SUPPLEMENTARY NOTES

19. KEY WORDS *(Continue on reverse side if necessary and identify by block number)*

Radiation damage; Single crystals of copper-aluminum alloys; Dislocation defects; Twins; Mechanical properties; Stress-strain relationships; Effects of strain rates; Cottrell-Stokes law

20. ABSTRACT *(Continue on reverse side if necessary and identify by block number)*

The ability of a reentry vehicle to sustain the radiation effects of a near nuclear burst and to successfully complete its mission depends to a large measure on the resulting damage to the loadbearing structural shell. To determine what changes in mechanical properties resulted from the exposure of copper-aluminum alloys to the intense radiation of a nuclear device, the yield strength, dislocation densities, changes in strain-rate, Young's Modulus, strain-rate sensitivity factor, Cottrell-Stokes ratio, and work hardening mechanisms were

DD FORM 1473 EDITION OF 1 NOV 65 IS OBSOLETE

studied as a function of radiation damage in single crystals of these alloys, which were tensile tested after nuclear exposure. The results of this program could influence input information used in our future prediction capabilities of fratricide against our own vehicles and in suggesting new hardening concepts which can increase the survivability of our future reentry vehicles.

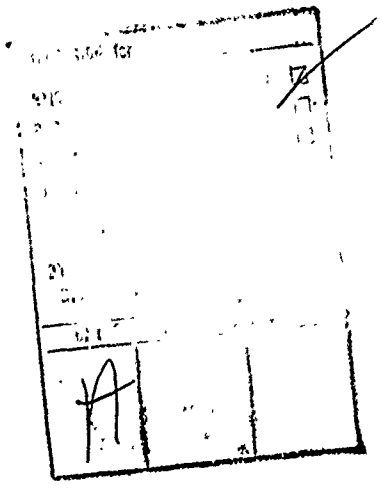

CONTENTS

Section		Page
I	INTRODUCTION	5
II	ENVIRONMENTAL APPROACH	6
	Dislocation Density Determination	6
	Tensile Properties	8
III	RESULTS	12
	Dislocation Distribution	12
	Tensile Properties of Irradiated Samples	22
IV	DISCUSSION	35
V	CONCLUSIONS	42
	REFERENCES	43

ILLUSTRATIONS

Figure		Page
1	Schematic Drawing Indicating Cutting of Tensile Specimens and Transmission Electron Microscopy Samples from Solid Radiation Coupons	7
2	Details of Tensile Specimen in Flexible Holder	9
3	Computer Controlled, Closed-Look Tensile Testing Apparatus	10
4	Typical Slip Band Development after Tensile Testing of Single Crystal Copper-Aluminum Alloys	11
5	Pressure versus Distance into Sample	13
6	Transmission Electron Micrograph of Shock-Loaded Pure Copper, 0.06 inch below the Incident Surface	14
7	Transmission Electron Micrograph of Shock-Loaded Pure Copper, 0.10 inch below the Incident Surface	15
8	Transmission Electron Micrograph of Shock-Loaded Pure Copper, 0.18 inch below the Incident Surface	16
9	Transmission Electron Micrograph of Shock-Loaded Copper-5 Percent Aluminum, 0.06 inch below the Incident Surface	17
10	Transmission Electron Micrograph of Shock-Loaded Copper-5 Percent Aluminum, 0.10 inch below the Incident Surface	18
11	Transmission Electron Micrograph of Shock-Loaded Copper-5 Percent Aluminum, 0.18 inch below the Incident Surface	19
12	Dark Field Transmission Electron Micrograph of Shock-Loaded Copper-5 Percent Aluminum, 0.06 inch below the Incident Surface--g=111	20
13	Dislocation Density versus Distance into Sample	21
14	True Stress versus True Strain for Copper-2.5 Percent Aluminum Alloy	23
15	True Stress versus True Strain for Copper-7 Percent Aluminum Alloy	24
16	Yield Stress versus Distance into Sample	25
17	Yield Stress versus the Square Root of the Dislocation Density	26

ILLUSTRATIONS (Continued)

Figure		Page
18	Strain Rate Sensitivity versus Strain for Pure Copper	27
19	Strain Rate Sensitivity versus Shear Stress for Copper and Copper-2.5 Percent Aluminum	28
20	Strain Rate Sensitivity versus Strain for two Copper-7 Percent Aluminum Alloys	29
21	Strain Rate Sensitivity versus Strain for Copper-5 Percent Aluminum	30
22	Strain Rate Sensitivity versus Strain for Three Copper-2.5 Percent Aluminum Alloys	32
23	Strain Rate Sensitivity versus Strain for Pure Copper and two Copper-7 Percent Aluminum Alloys	33
24	Cottrell-Stokes Parameter versus Strain	34
25	Copper-7 Percent Aluminum 3B1, Tensile Strained 8.4 Percent after Shock Loading with Defraction Patterns Showing Twin Spots (T) and Streaking (S) Due to Thin Stacking Faults	40
26	Copper-7 Percent Aluminum 3B1, Tensile Strained 8.4 Percent after Shock Loading with Defraction Patterns Showing Twin Spots (T) and Streaking (S) Due to Thin Stacking Faults	41

SECTION I

INTRODUCTION

The ability of a reentry vehicle to sustain the radiation effects of a near nuclear burst and then to successfully complete its mission depends to a large measure on the resulting strength of the structural shell of the vehicle. A 3-year comprehensive and fundamental in-house experimental program was carried out at the Air Force Weapons Laboratory (AFWL) to determine what changes in the mechanical properties of several reentry vehicle-like materials resulted from their exposure to an actual underground nuclear burst. An important goal of this research was the assessment of fratricide possibilities from our own multiple warheads and the hardening of our vehicles against the antiballistic missiles of the enemy. A major question resolved by this work was whether or not reentry vehicle metal shells could maintain their structural strength despite surface melting and blow-off from the intense nuclear radiation. It is suggested that the experimental results of this program have a marked impact on inputs to our failure prediction capabilities, as well as suggesting new hardening concepts which could increase the survivability of future reentry vehicle systems.

SECTION II

ENVIRONMENTAL APPROACH

Thirty-two aluminum, copper, and nickel alloys were exposed to the intense radiation of a recent underground test. However, in this report only copper and copper-aluminum alloy results will be reported. Very pure copper (99.9999 percent), copper-2.5 percent aluminum, copper-5 percent aluminum, and copper-7 percent aluminum were momentum-trapped with like material so that only the compressive portion of the shock wave produced by the incident radiation was transmitted through each sample. All of the metal samples were single crystals to eliminate the radiation complexities of impurity content at grain boundaries on the resultant mechanical properties of these materials. In addition, all of the samples were oriented such that the incident radiation was along the [111] direction in each of the crystals. The specimens were 1/4 inch thick and 7/8 inch in diameter. After the samples were recovered from the nuclear tests, they were sectioned parallel to their front surface every 0.04 inch by a Servomet electric spark erosion machine. From these slices, small tensile specimens and transmission electron microscopy samples were electro-spark machined, electropolished, and tested (figure 1).

1. DISLOCATION DENSITY DETERMINATION

Transmission electron microscopy samples from near the gauge portion were thinned in a standard electropolishing solution to 2000 Å and examined in a 100-kV microscope on a double tilting stage. Dislocation densities were calculated by (1) determining the thickness of the foils by measuring the width of dislocation traces and stacking faults and (2) utilizing electron diffraction patterns of each sample to determine the foil orientation. The intersection analysis technique of Smith and Guttman (ref. 1) was carried out. The problem of the dislocation density being affected by local rotation of the dislocations in the foil which produces a nonrandom, low value of the density was overcome by using a series of circles instead of random straight lines, after Steeds (ref. 2). A two-beam condition was always used in taking each of the transmission photographs so that the percentage of invisible dislocations could be calculated following Hirsch et al. (ref. 3). Great care was exercised in selecting areas of each sample which truly represented typical dislocation

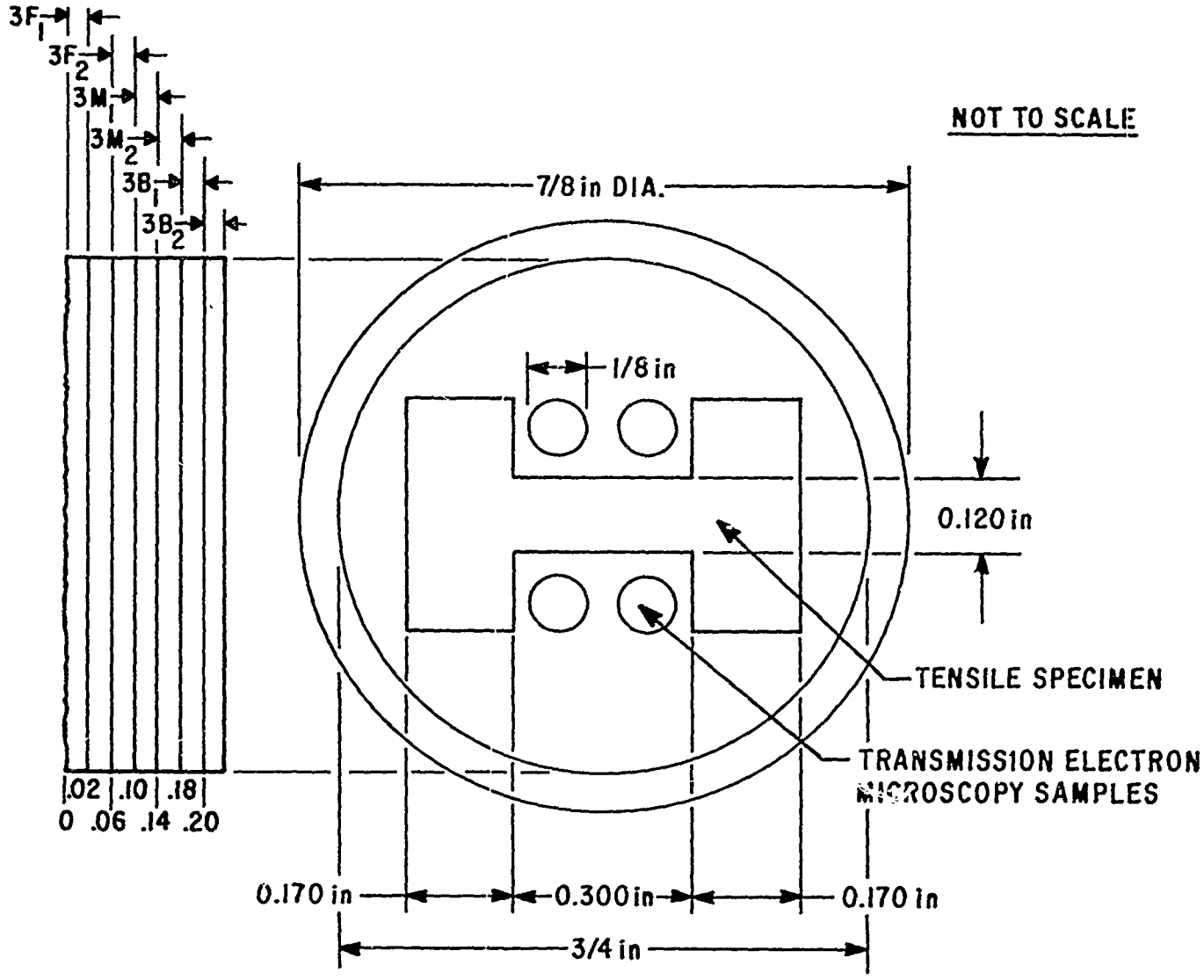

Figure 1. Schematic Drawing Indicating Cutting of Tensile Specimens and Transmission Electron Microscopy Samples from Solid Radiation Coupons

densities. As a result, hundreds of pictures were taken for each alloy series. Additional confidence that the reported dislocation densities represent the actual shock-loaded state is gained by realizing that the nuclear radiation which produces the dislocations simultaneously pins them in place by vacancies and vacancy clusters, also created by the radiation.

2. TENSILE PROPERTIES

Each of the slices from each sample exposed in the underground test was electrospark machined into a tensile specimen. Following this, each tensile specimen was carefully electropolished to remove any damage from the electrospark machining process. Typical dimensions of the tensile specimens, whose thickness ranged from about 0.015 to 0.020 inch, are shown in figure 1. These small tensile specimens were mounted in a special gripping device consisting of a series of gimbaled pinning fixtures that allowed for complete freedom from bending of the samples and assured proper alignment in the grips during tensile testing (figure 2). The tensile tests were carried out in an MTS, hydraulically operated, closed loop feedback tensile tester similar to the one shown in figure 3. The apparatus consists of a slave computer which is used both to control the tensile tests at constant strain rates and to analyze the data. As many as 15 different changes in the strain-rate can be imposed on the sample during a test. These strain-rate changes are used to simulate the sudden momentum changes and changes in stress induced in a reentry vehicle during evasive maneuvering. The orientation of each of the crystals tested was such that the face of the tensile specimen was the (111) plane and the [$\bar{1}\bar{1}$1] direction was at approximately 45° to the tensile direction. One such slip system can be clearly seen in figure 4 which shows a tensile specimen of pure unirradiated copper after an elongation of approximately 8.5 percent. Analysis of the tensile test results was carried out to determine the yield stress, the increase in stress required for specific increase in strain rate and a measure of the rate of work hardening as a function of both the position of each sample within the 1/4-inch irradiated specimen and the dislocation density.

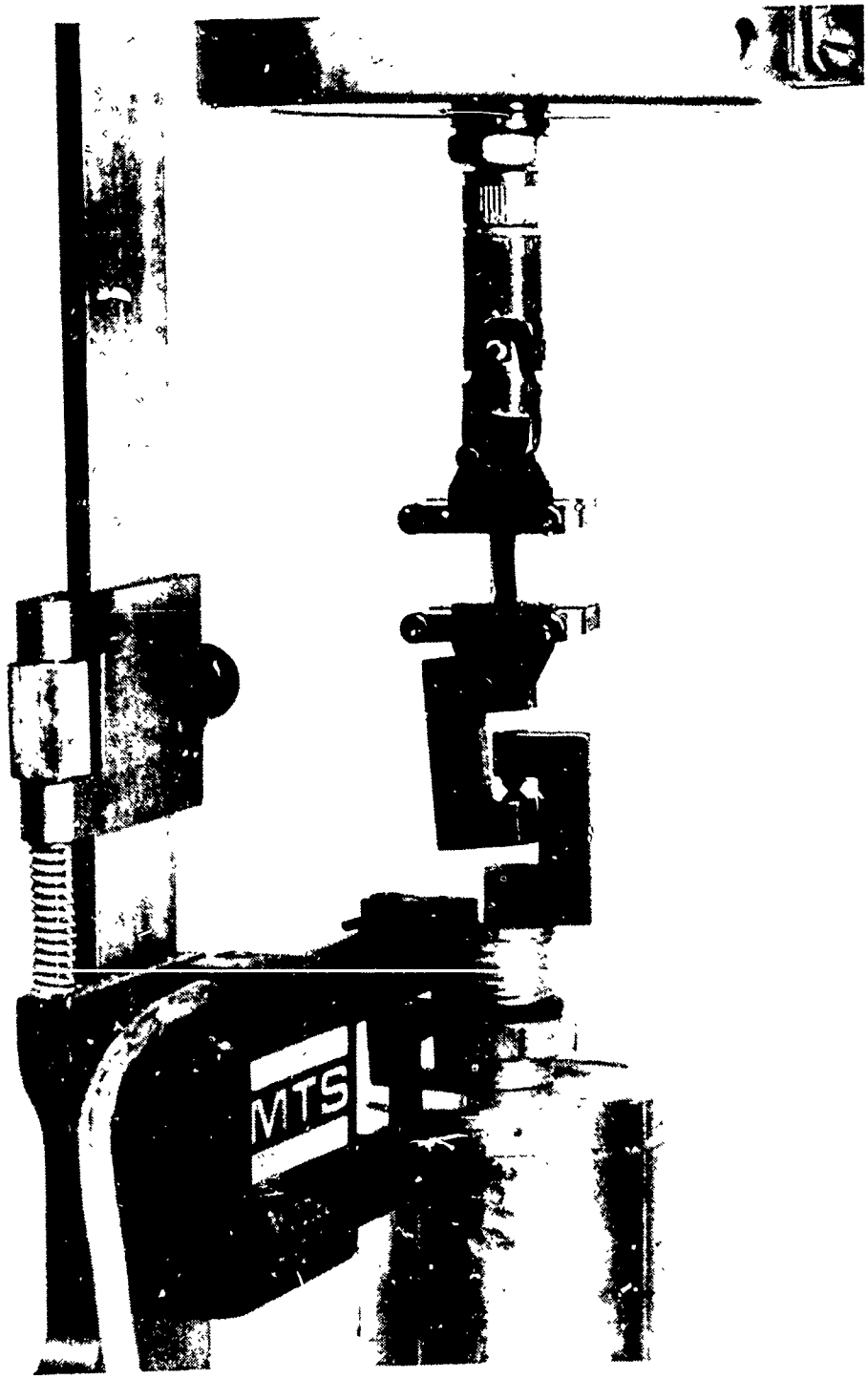

Figure 2. Details of Tensile Specimen in Flexible Holder

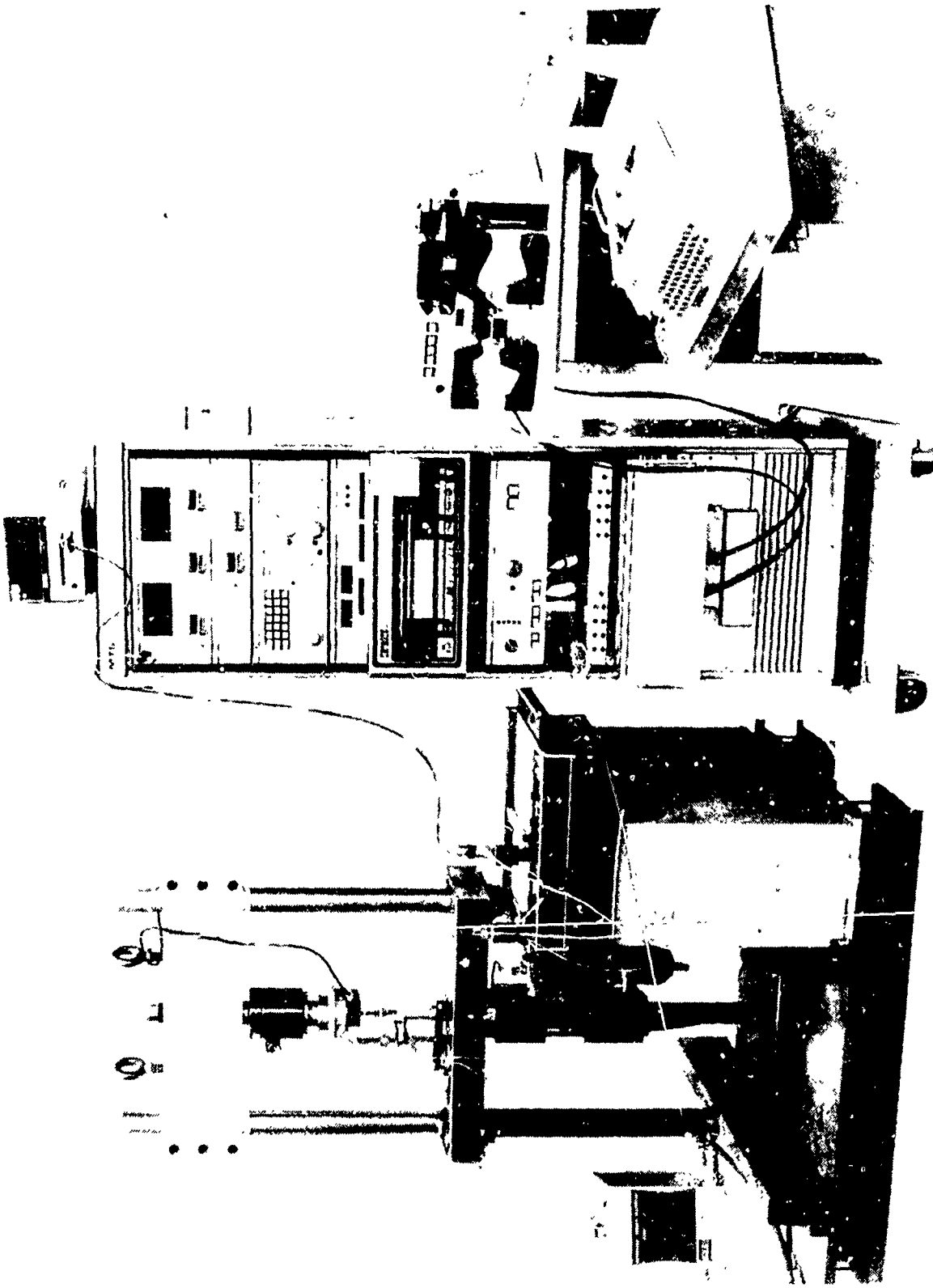

Figure 3. Computer Controlled, Closed-Look Tensile Testing Apparatus

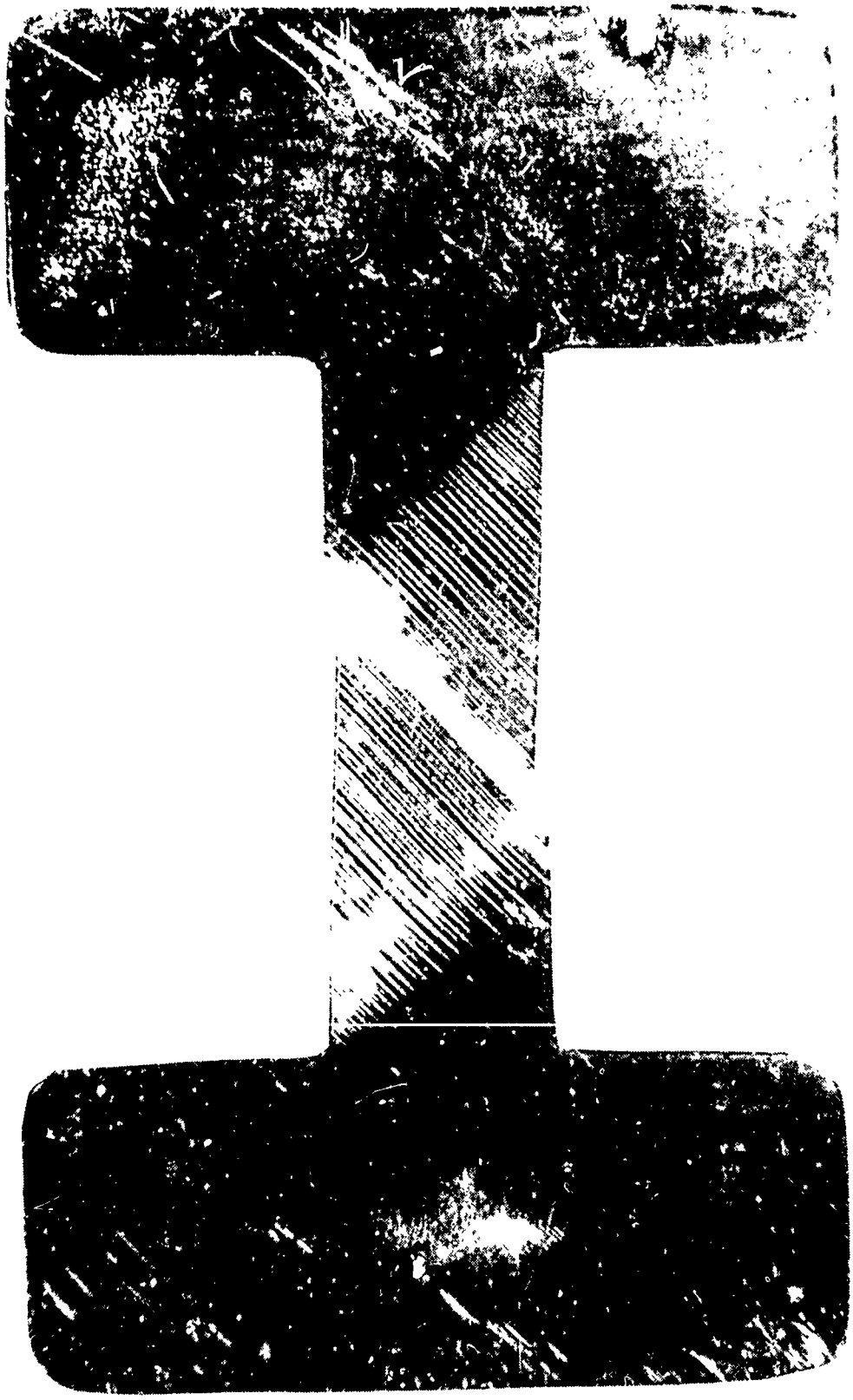

Figure 4. Typical Slip Band Development after Tensile Testing of Single Crystal Copper-Aluminum Alloys (Gage Length Approximately 0.3 inch)

SECTION III

RESULTS

1. DISLOCATION DISTRIBUTION

Figure 5 is a plot of the calculated pressure produced by radiation-induced blow-off versus distance into pure copper, showing the exponential decay of the stress due to attenuation by the thickness of the sample. The resulting defects produced in the pure copper and in the copper-aluminum alloys are shown in figures 6 through 11. The radiation damage manifests itself in the production of dislocations (the line defects shown in these figures) and in vacancy clusters (the point defects seen in between the dislocation agglomerations). Figures 6, 7, and 8 show typical transmission electron micrographs for pure copper at 0.06 inch, 0.10 inch, and 0.018 inch below the incident surface, respectively. Figures 9, 10, and 11 show typical transmission electron micrographs of the shock-loaded copper-5 percent aluminum sample at 0.06 inch, 0.10 inch, and 0.018 inch below the incident surface. Note the decrease in both the dislocation density and the number of point defects as a function of depth below the front surface. In figure 9, because of the lowering of the stacking fault energy of copper by aluminum additions, faults are created during shock loading which are seen to run along the [110] directions at angles of 60° to each other. The nature of these faults was determined to be of the extrinsic type by use of dark field electron microscopy. Figure 12 shows extrinsic areas, indicated by the letter "E." These faults disappear in the copper-5 percent aluminum alloy at a distance of 0.10 inch below the incident surface. For example, in the lower left-hand corner of figure 10, a stacking fault is just barely visible; compare with figure 11 in which stacking faults are absent. Comparison with figure 5 indicates that the critical pressure requisite to induce stacking faults in the copper-5 percent aluminum alloys is 50 kilobars. This fact can be used to calibrate passive metal gauges in an underground test. Figure 13 shows the dislocation densities for pure copper, copper-2.5 percent aluminum, and copper-5 percent aluminum, as a function of distance into each of the samples, determined from these transmission electron microphotographs. It is interesting to note that in the pure copper as well as in the copper-5 percent aluminum samples that the maximum dislocation density does not occur

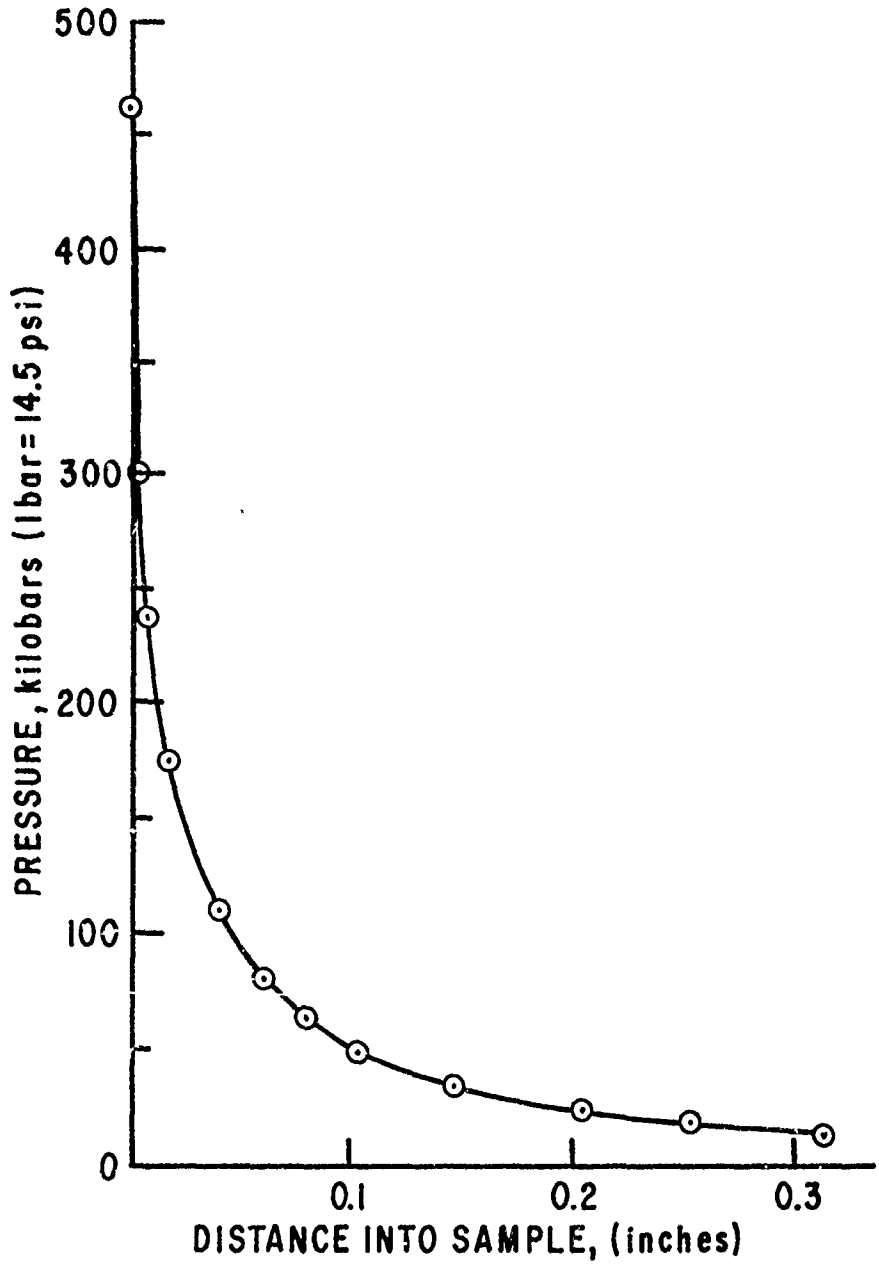

Figure 5. Pressure versus Distance into Sample

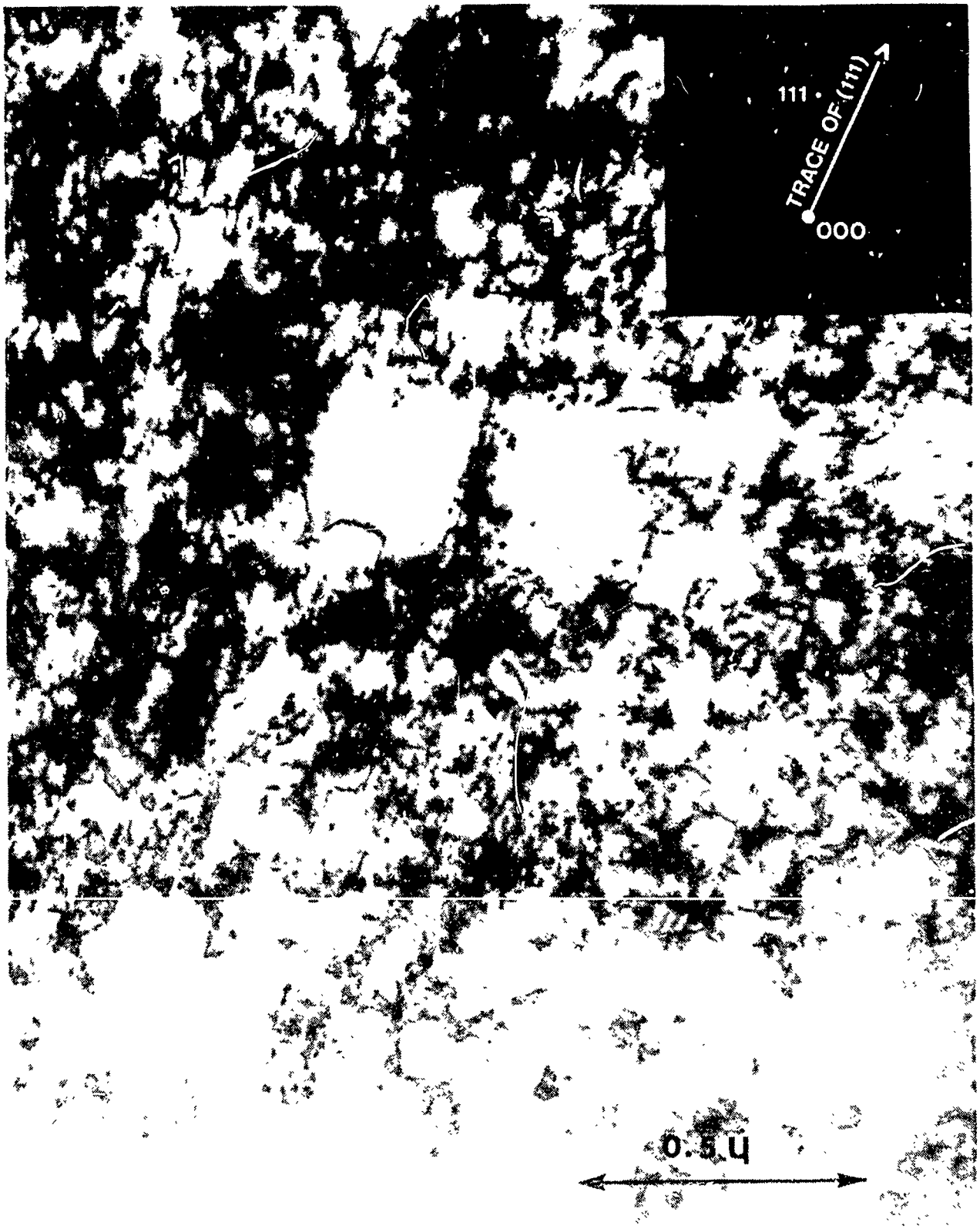

Figure 6. Transmission Electron Micrograph of Shock-Loaded Pure Copper, 0.0[illegible] Inch below the Incident Surface

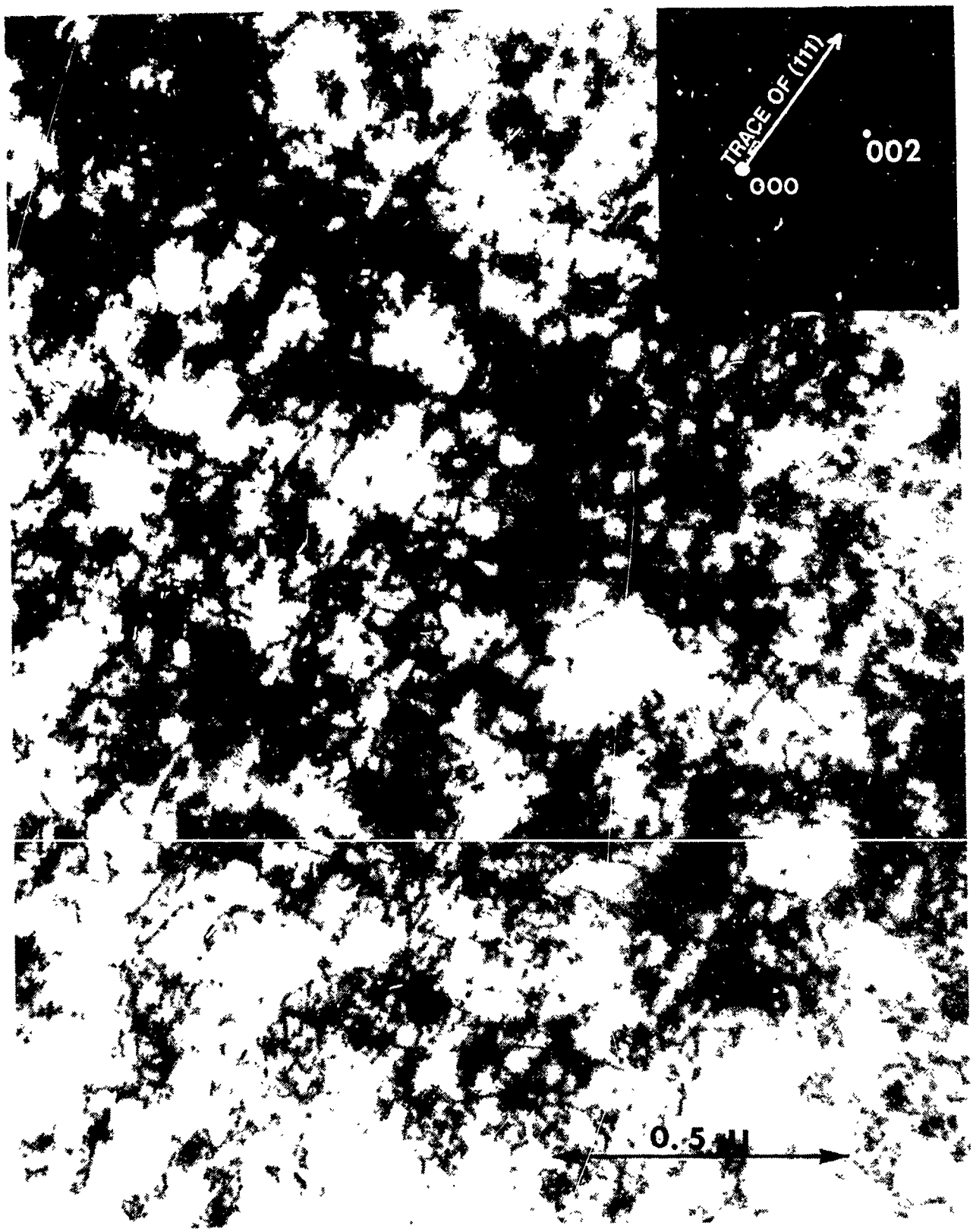

Figure 7. Transmission Electron Micrograph of Shock-Loaded Pure Copper, 0.10 Inch below the Incident Surface

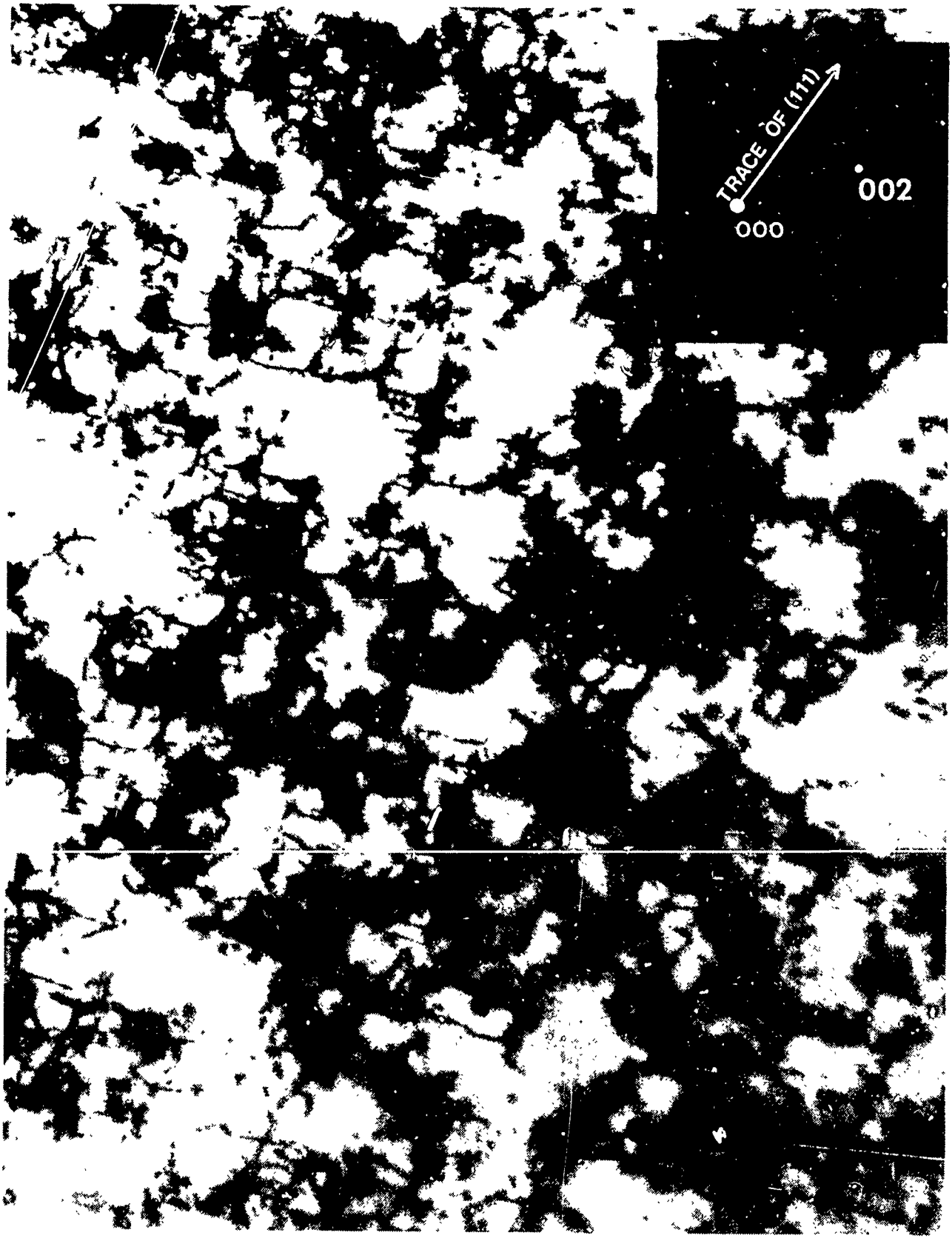

Figure 8. Transmission Electron Micrograph of Shock-Loaded Pure Copper, 0.18 Inch below the Incident Surface

Figure 9. Transmission Electron Micrograph of Shock-Loaded Copper-5 Percent Aluminum, 0.06 Inch below the Incident Surface

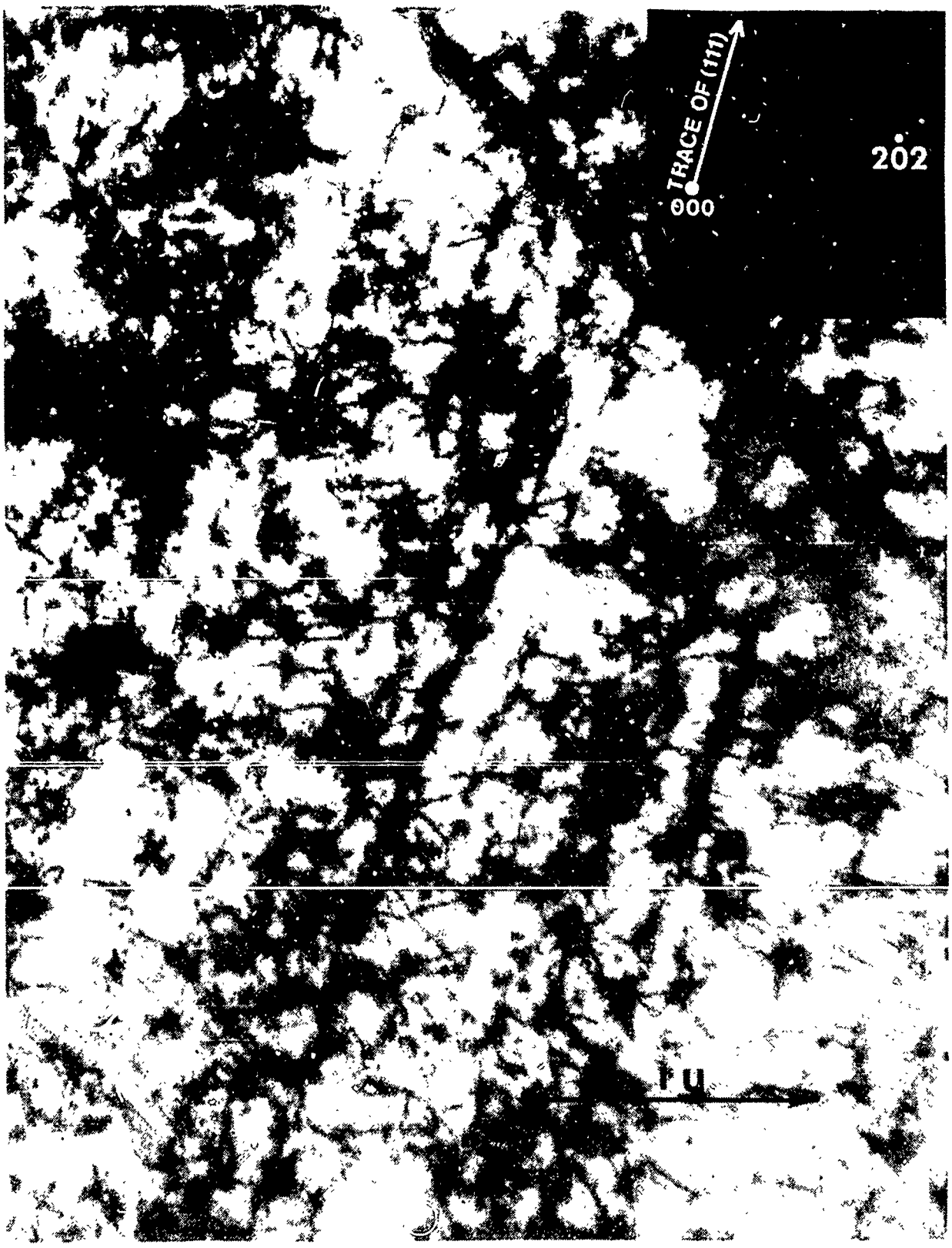

Figure 10. Transmission Electron Micrograph of Shock-Loaded Copper-5 Percent Aluminum, 0.10 Inch below the Incident Surface

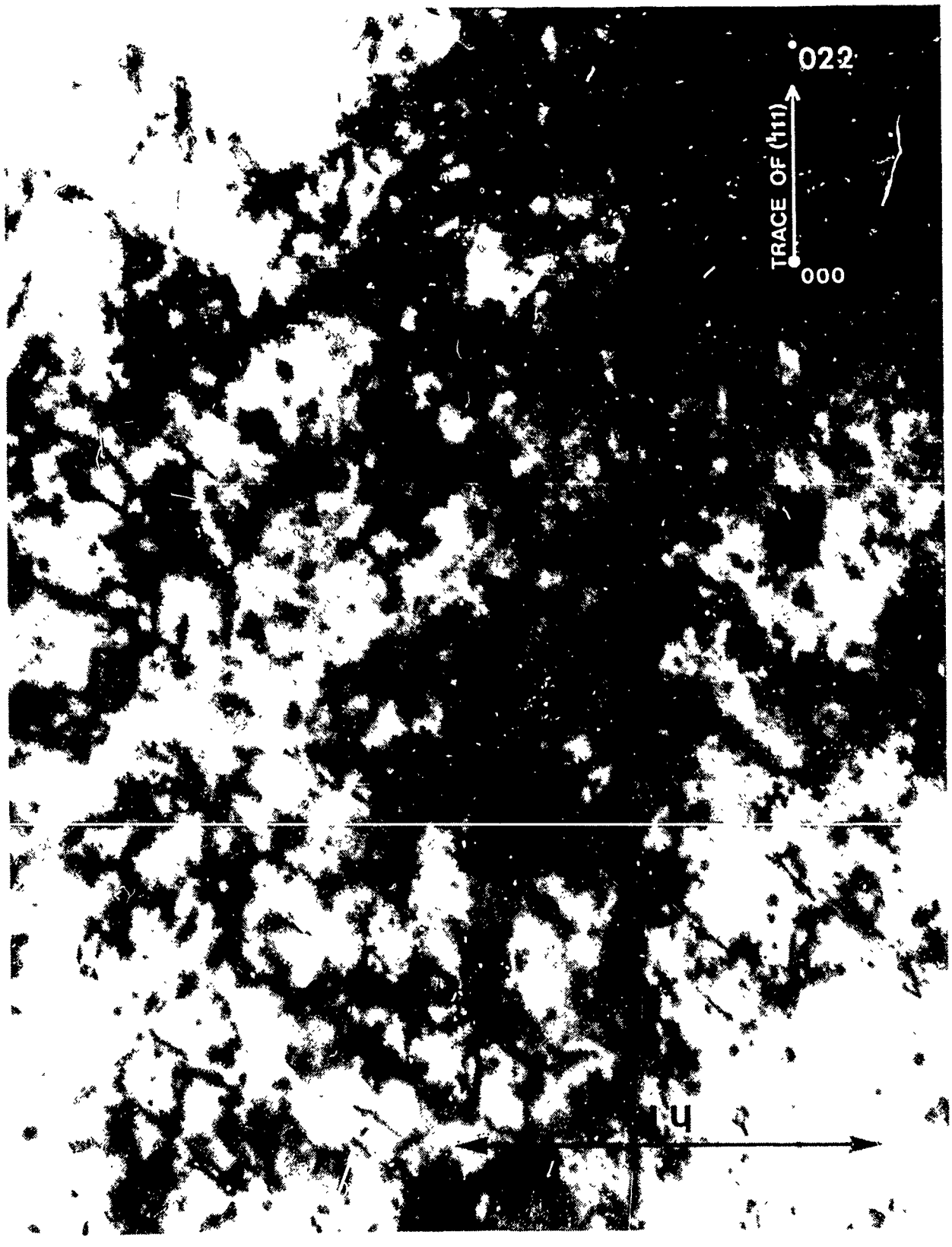

Figure 11. Transmission Electron Micrograph of Shock-Loaded Copper-5 Percent Aluminum, 0.18 Inch below the Incident Surface

Figure 12. Dark Field Transmission Electron Micrograph of Shock-Loaded Copper-5 Percent Aluminum 0.06 Inch below the Incident Surface--g=111 (Extrinsic faults are marked)

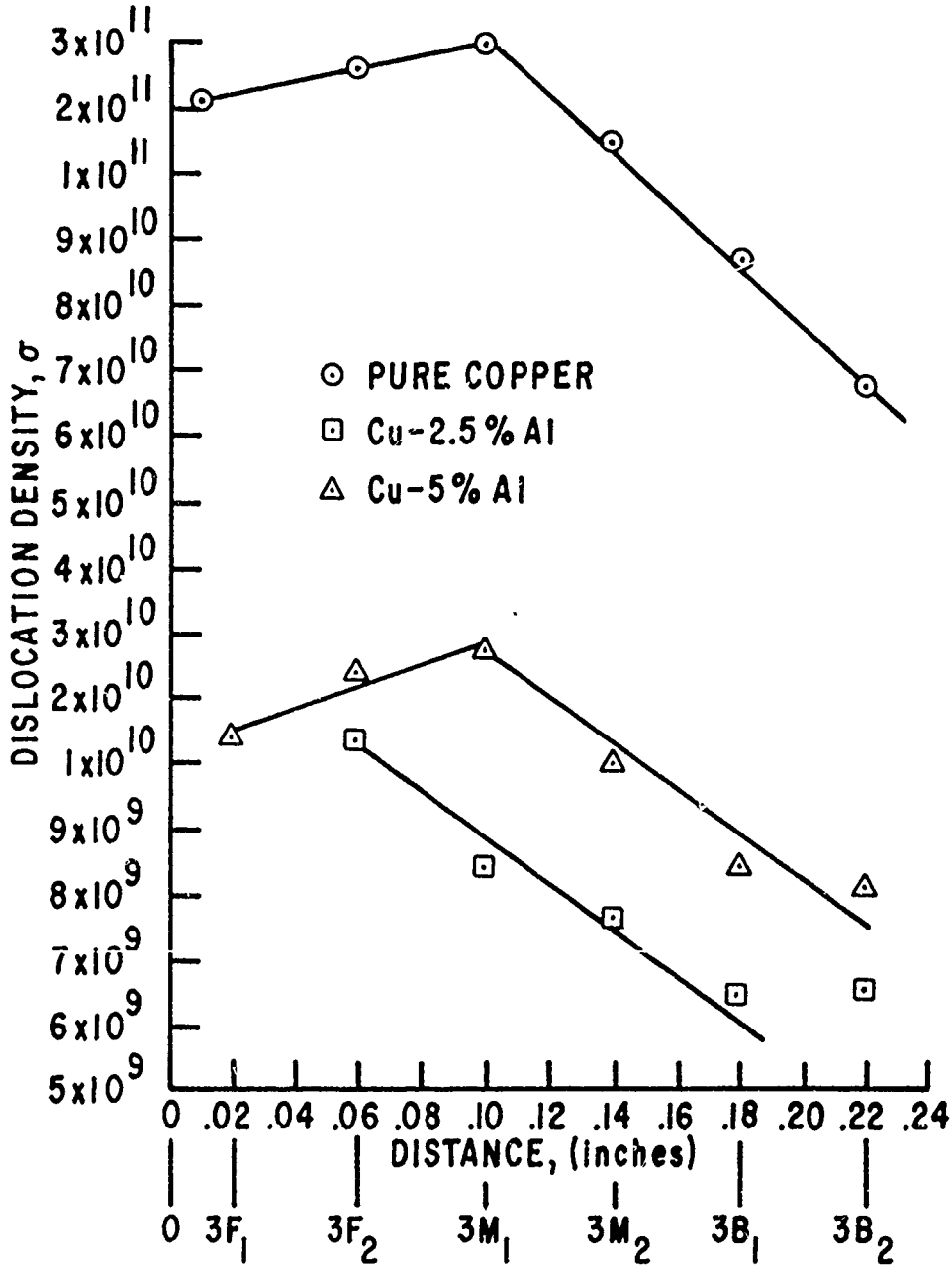

Figure 13. Dislocation Density versus Distance into Sample

within the first slice (3F1), which is 0.02 inch below the incident surface, but at a distance of 0.10 inch below the surface. In these samples it is felt that the dislocation density near the surface was decreased due to the melting at the front surface. Figure 13 shows that for these three alloys a straight line relationship exists between the dislocation density and distance into the sample below the middle slice (3M1). The effect of these dislocation densities on the mechanical properties of these alloys was determined and is reported below.

2. TENSILE PROPERTIES OF IRRADIATED SAMPLES

From the many tensile tests conducted on copper and copper alloys, two typical true stress versus true strain curves are shown in figures 14 and 15 for copper-2.5 percent aluminum and for copper-7 percent aluminum, respectively. Figure 14 shows seven alternating changes in the strain rate between 0.01 inch per inch per minute and 1.0 inch per inch per minute occurring between 1 percent and 6 percent of the true strain. In figure 15 progressive changes in the strain rate were made at 3 percent, 4 percent, 5 percent, and 6 percent true strain from 0.001 inch per inch per minute to 10.0 inches per inch per minute at these various values of true strain. For each of the tensile specimens tested, the following data were acquired: the yield stress, the elastic modulus, the change in stress required to execute the various changes in strain rates, and changes in the modulus due to the sudden changes in the strain rates. Figure 16 is a composite plot of the copper-aluminum alloys showing the variation of the yield stress versus the position from the front surface from which the tensile specimen was cut. For comparison purposes the value of the average of the yield stress of four unirradiated pure copper specimens is shown on the same figure at 6000 psi. Figure 17 shows the variation in the yield stress as a function of the dislocation density for pure copper, copper-2.5 percent aluminum, and copper-5 percent aluminum. A straight line dependency between the yield stress and the square root of the dislocation density is indicated for each of these curves, with the slope, α, indicated above each line.

The strain rate sensitivity factor, m', versus deformation for copper, copper-2.5 percent aluminum, copper-7 percent aluminum, and copper-5 percent aluminum are shown in figures 18, 19, 20, and 21, respectively. The strain rate sensitivity for the first three metals is seen to be independent of the deformation, while the strain rate sensitivity for copper-5 percent aluminum varies linearly with the strain. In each of these four plots, the upward or downward

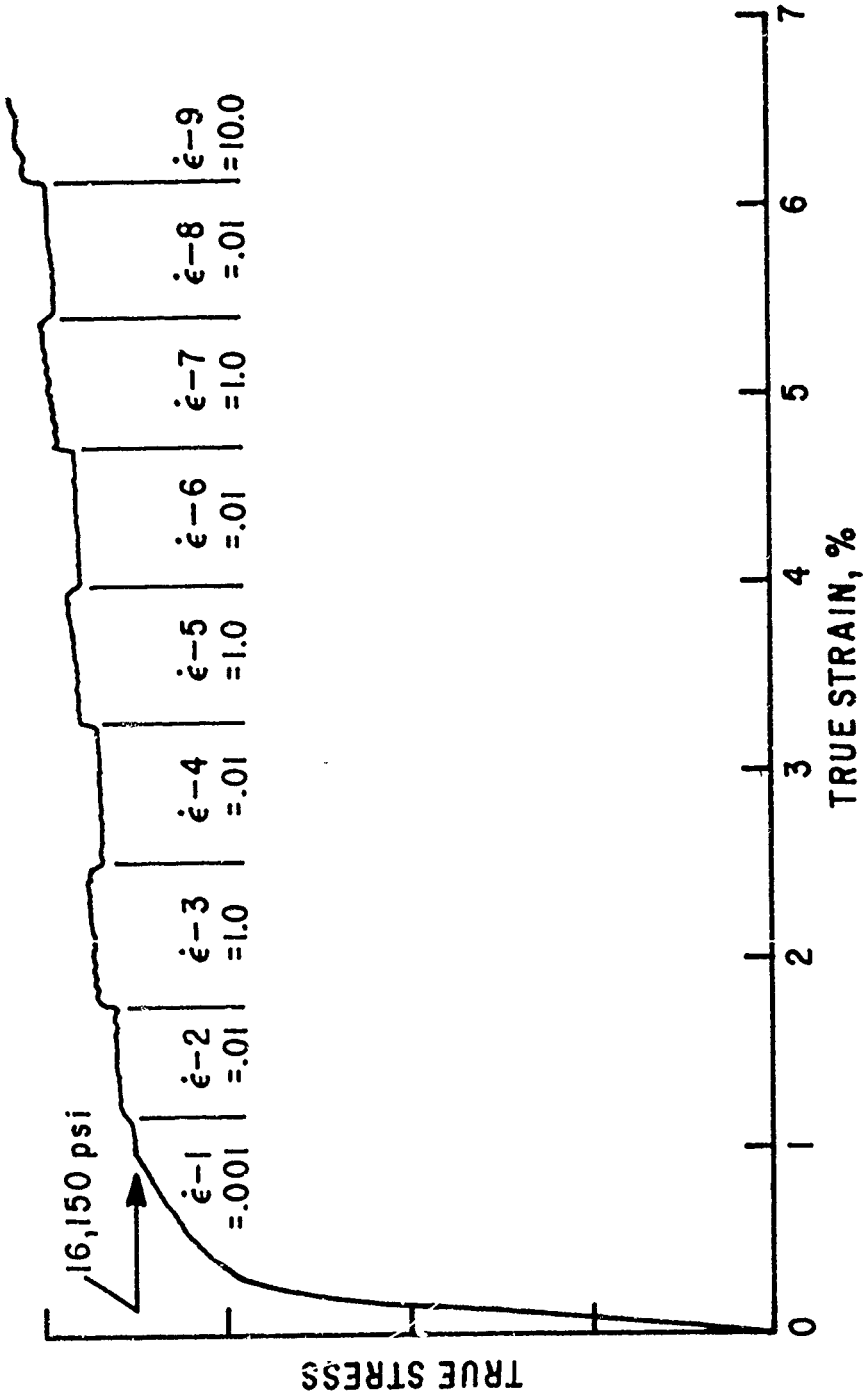

Figure 14. True Stress versus True Strain for Copper-2.5 Percent Aluminum Alloy

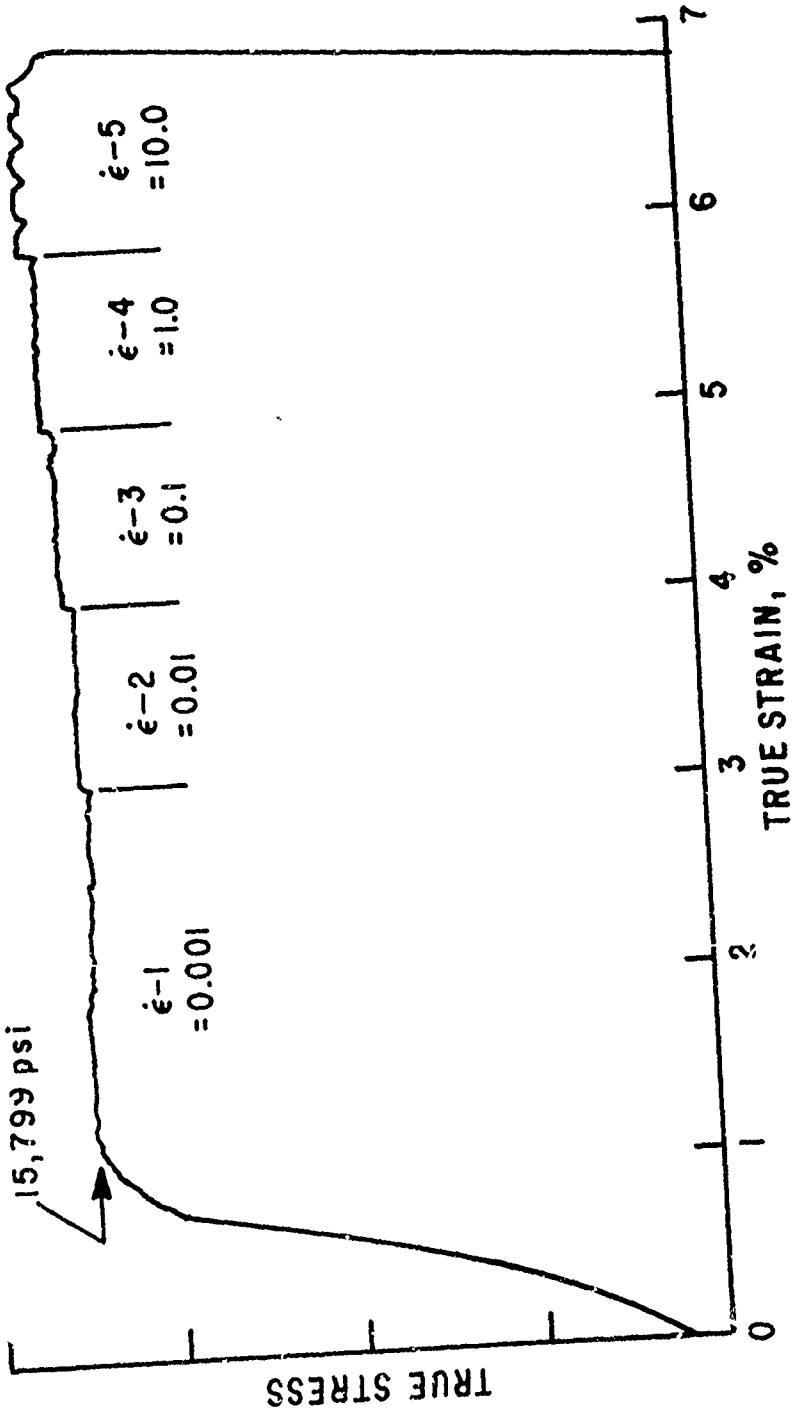

Figure 15. True Stress versus True Strain for Copper-7 Percent Aluminum Alloy

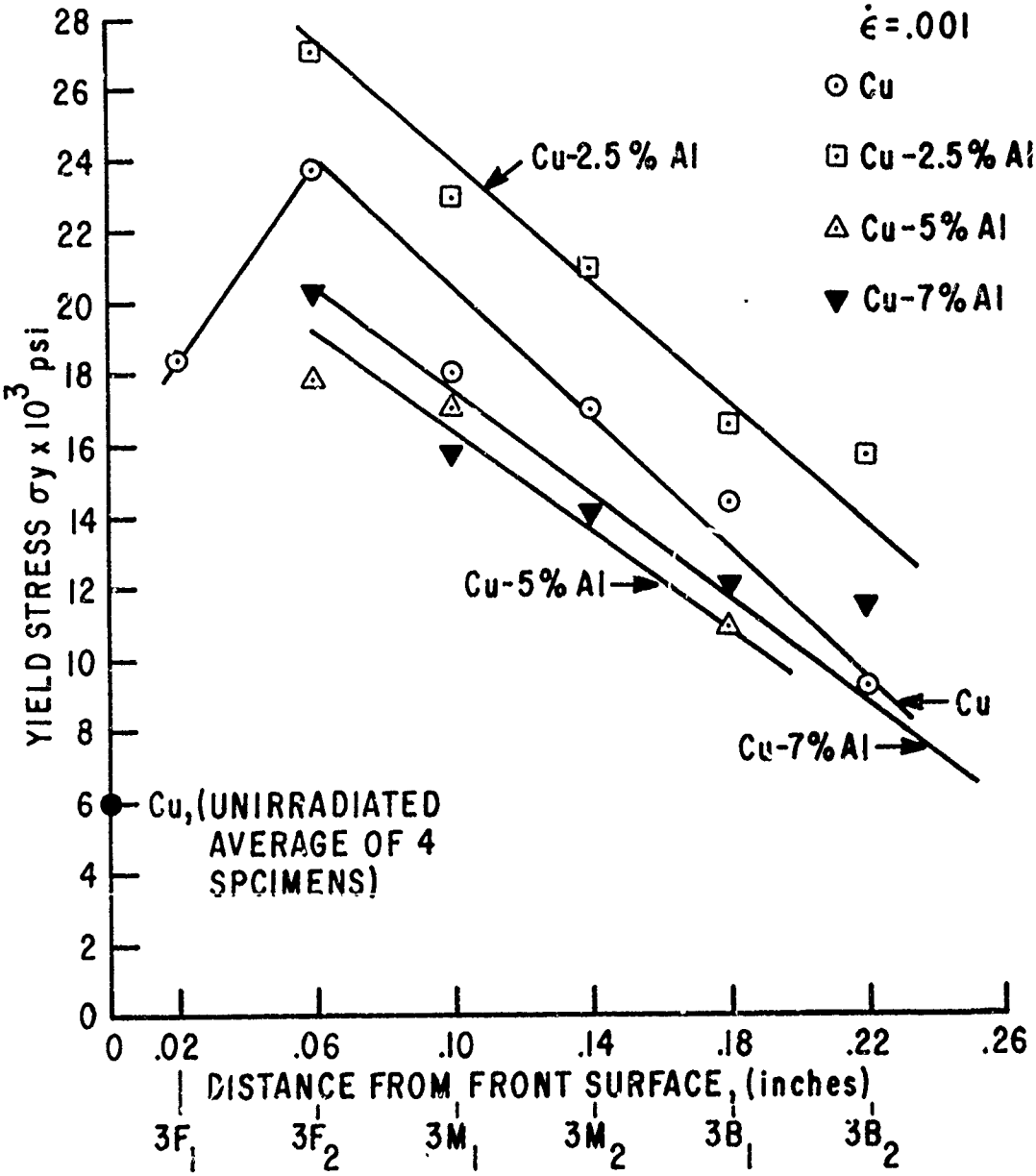

Figure 16. Yield Stress versus Distance into Sample

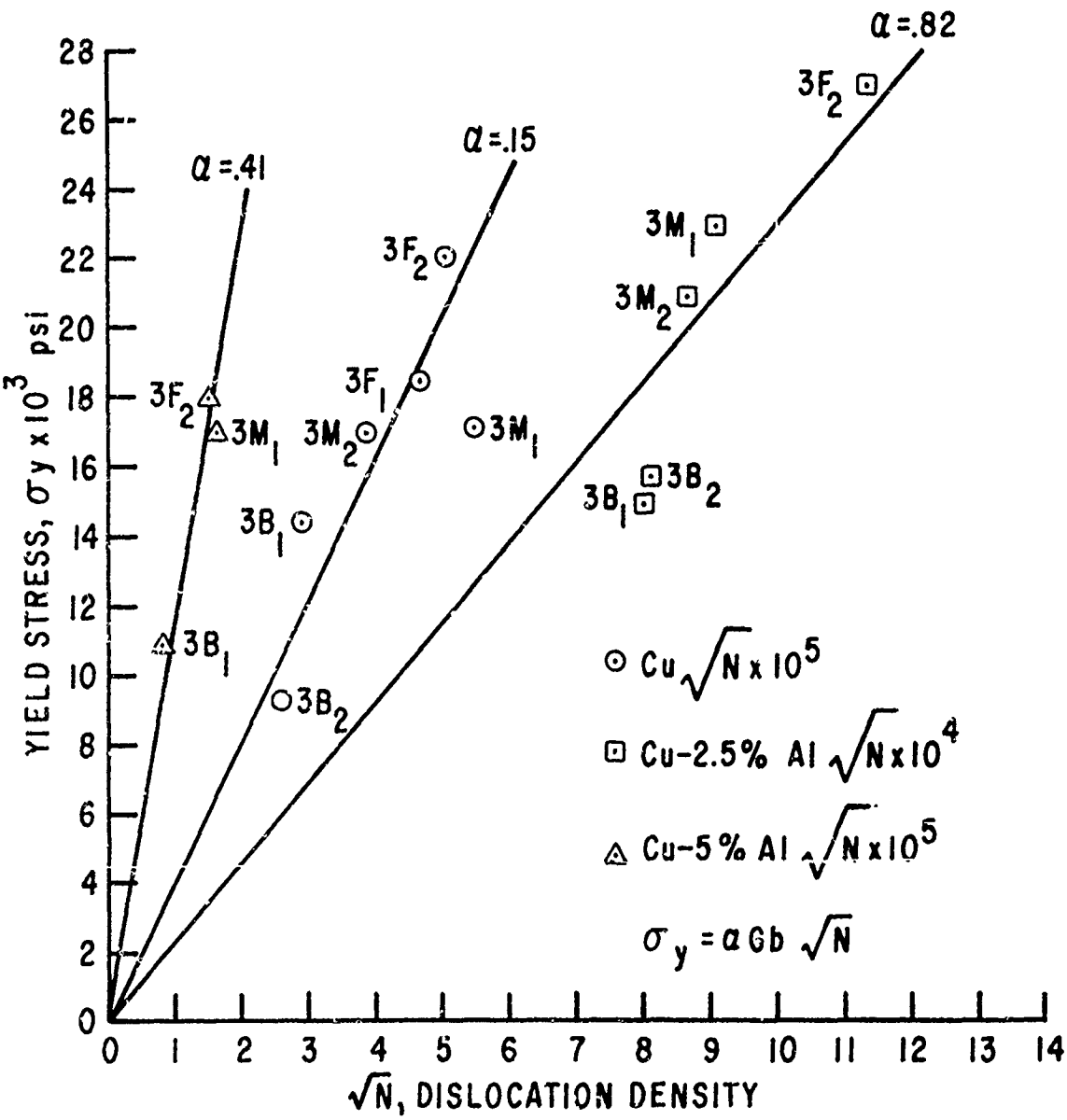

Figure 17. Yield Stress versus the Square Root of the Dislocation Density

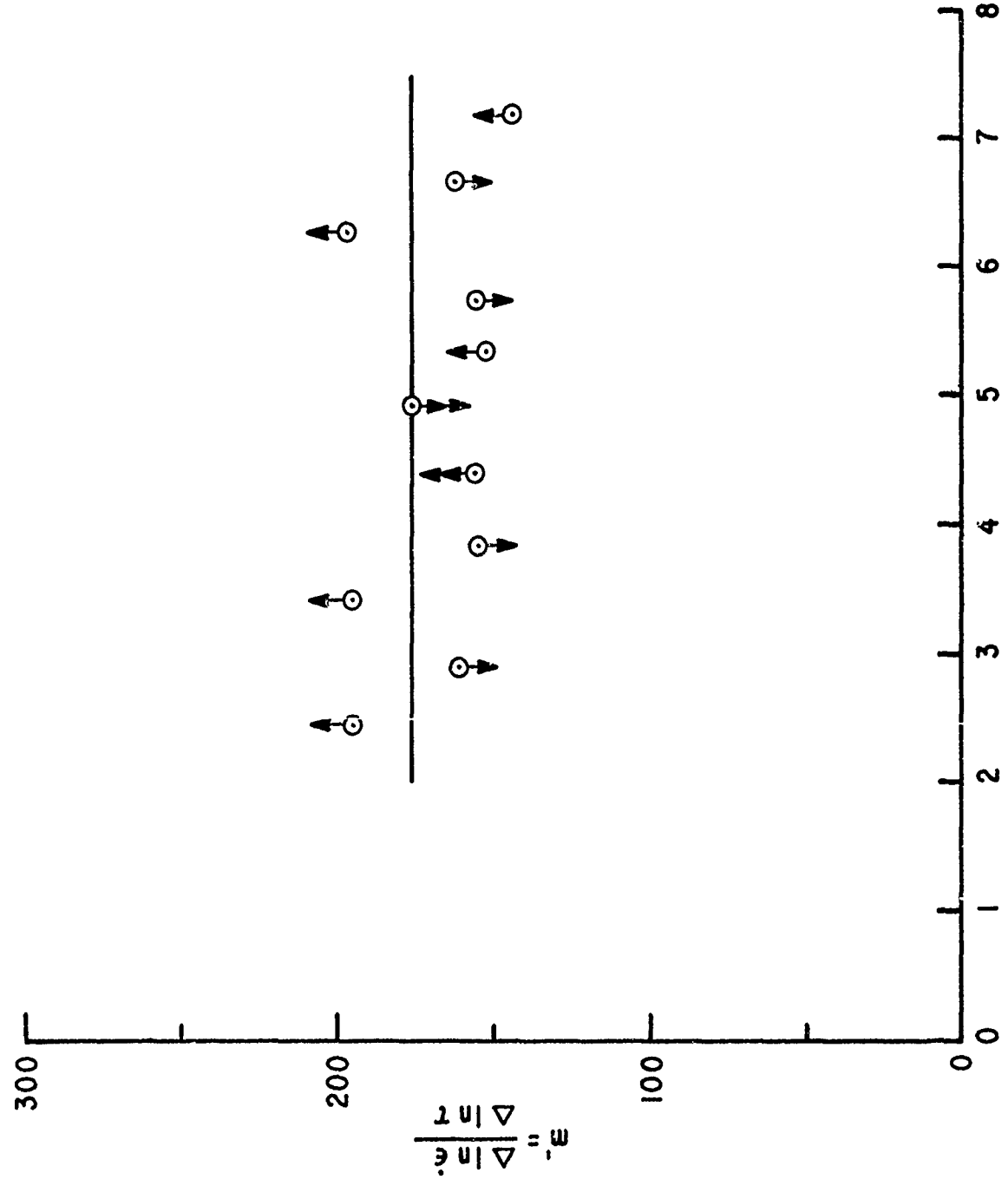

Figure 18. Strain Rate Sensitivity versus Strain for Pure Copper

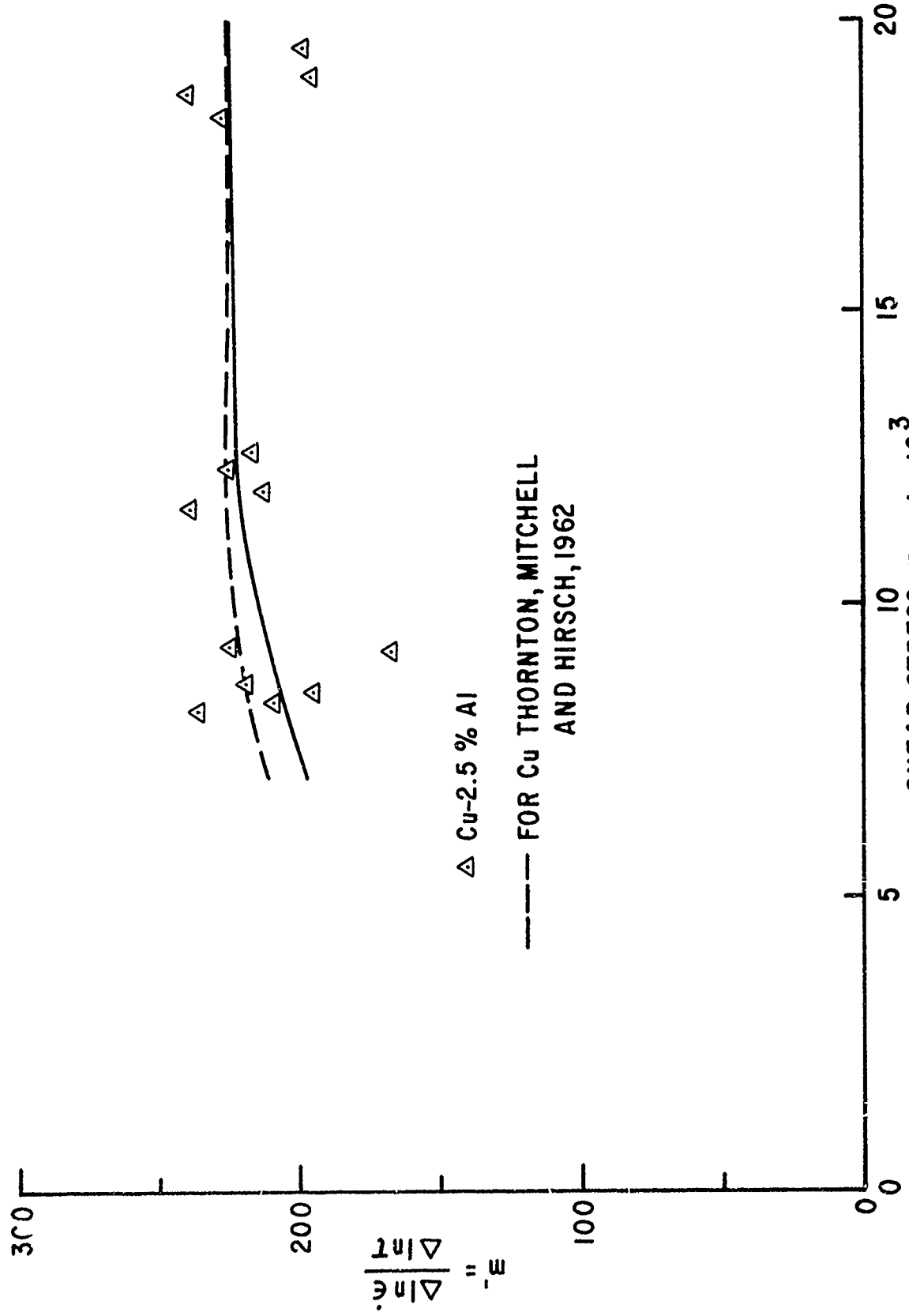

Figure 19. Strain Rate Sensitivity versus Shear Stress for Copper and Copper-2.5 Percent Aluminum

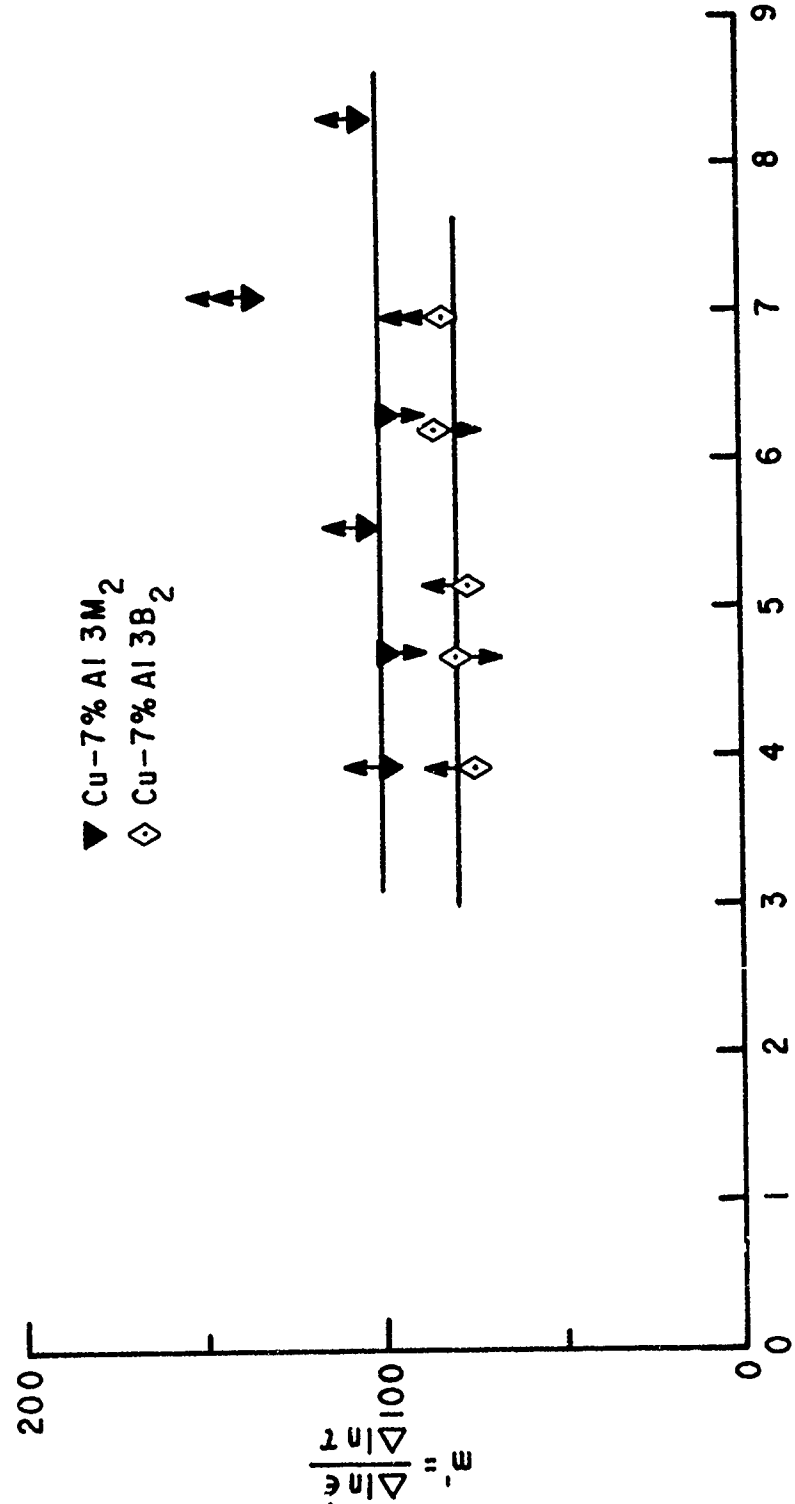

Figure 20. Strain Rate Sensitivity versus Strain for Two Copper-7 Percent Aluminum Alloys

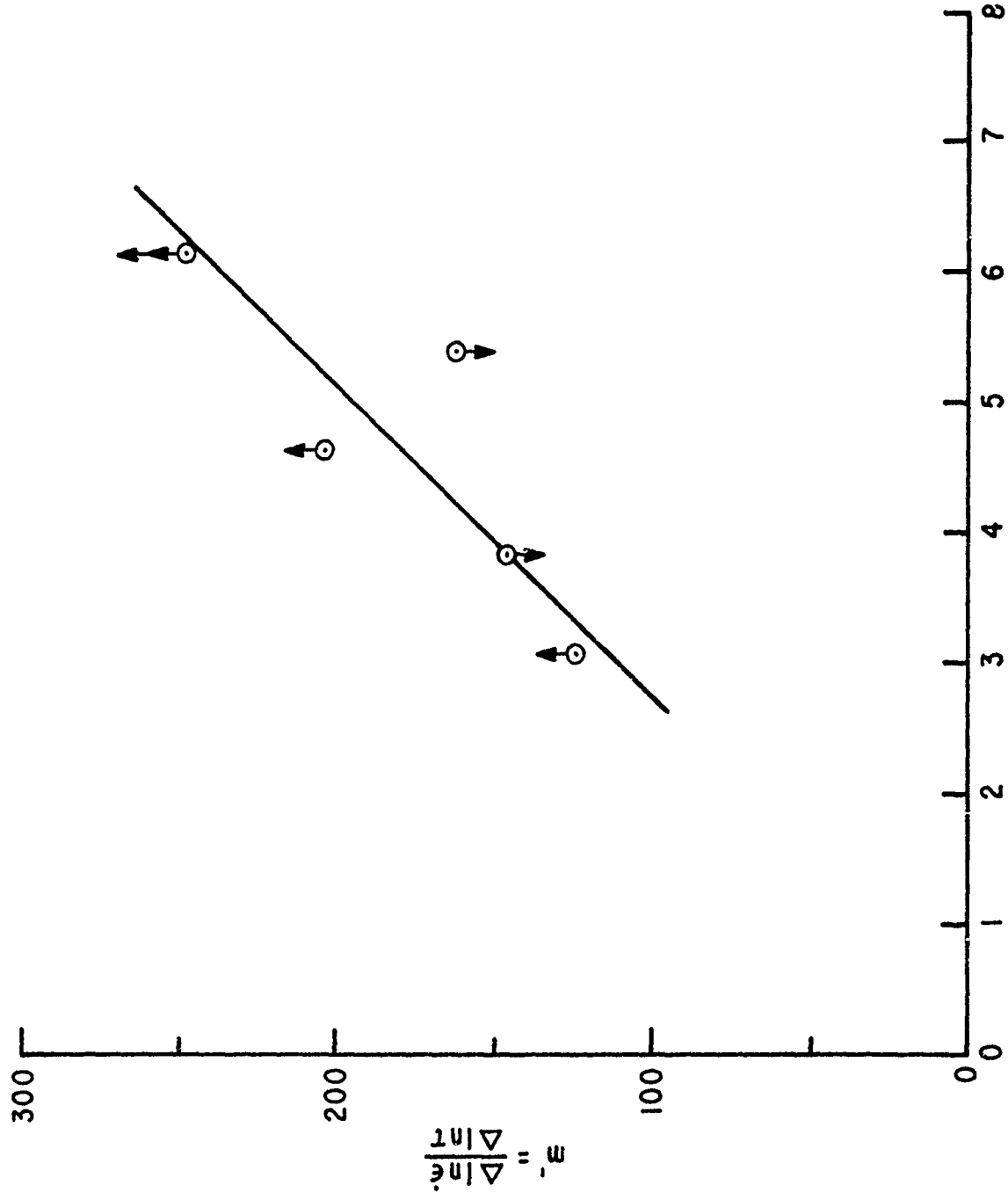

Figure 21. Strain Rate Sensitivity versus Strain for Copper-5 Percent Aluminum

pointing arrows indicate changes of two orders of magnitude in the strain rate from the same base strain rate of 0.1 inch per inch per minute, either for an increasing or a decreasing rate, respectively. The double arrows on points in these plots indicate three orders of change in the strain rate from 0.01 inch per inch per minute to 10 inches per inch per minute. Figures 22 and 23 show the variation in the strain rate sensitivity factor versus strain for copper-2.5 percent aluminum and copper-7 percent aluminum, respectively. In these plots the strain rate was changed successively by one order of magnitude starting from 0.001 inch per inch per minute until 10 inches per inch per minute was imposed on the tensile specimens. These figures show a linear dependency of the strain rate sensitivity factor with the strain which decreases as the strain rate increases.

Figure 24 is a plot of the Cottrell-Stokes parameter versus stress for several samples of copper-2.5 percent aluminum, copper-5 percent aluminum, and copper-7 percent aluminum. This figure shows that several specimens exhibit positive deviations from the Cottrell-Stokes law with approximately the same slope between the parameter and the shear stress at large values of the strain. On the other hand, for those copper-2.5 percent aluminum specimens in which changes in the strain rate were imposed at lower values of the strain, the Cottrell-Stokes law is essentially obeyed.

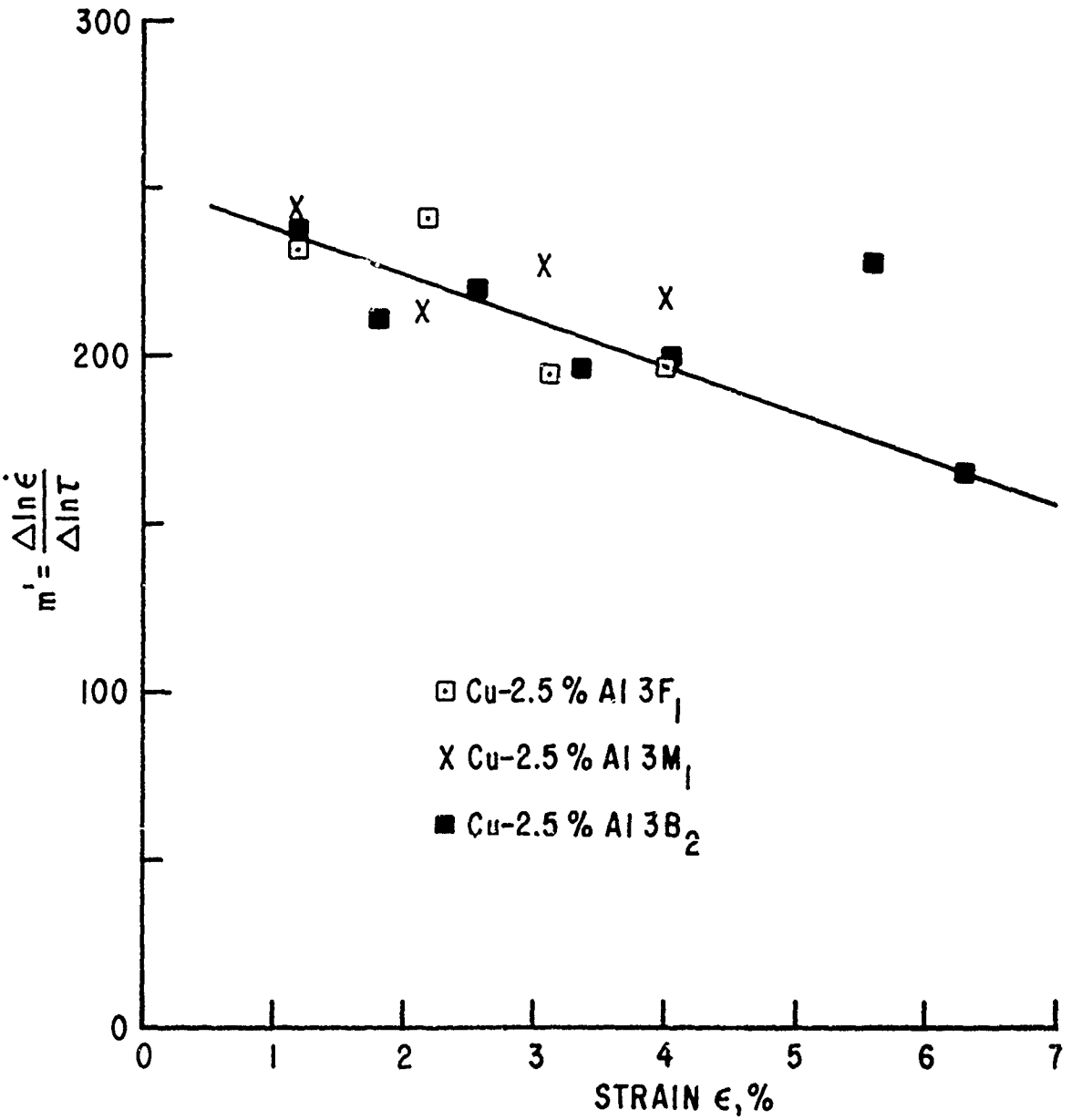

Figure 22. Strain Rate Sensitivity versus Strain for Three Copper-2.5 Percent Aluminum Alloys

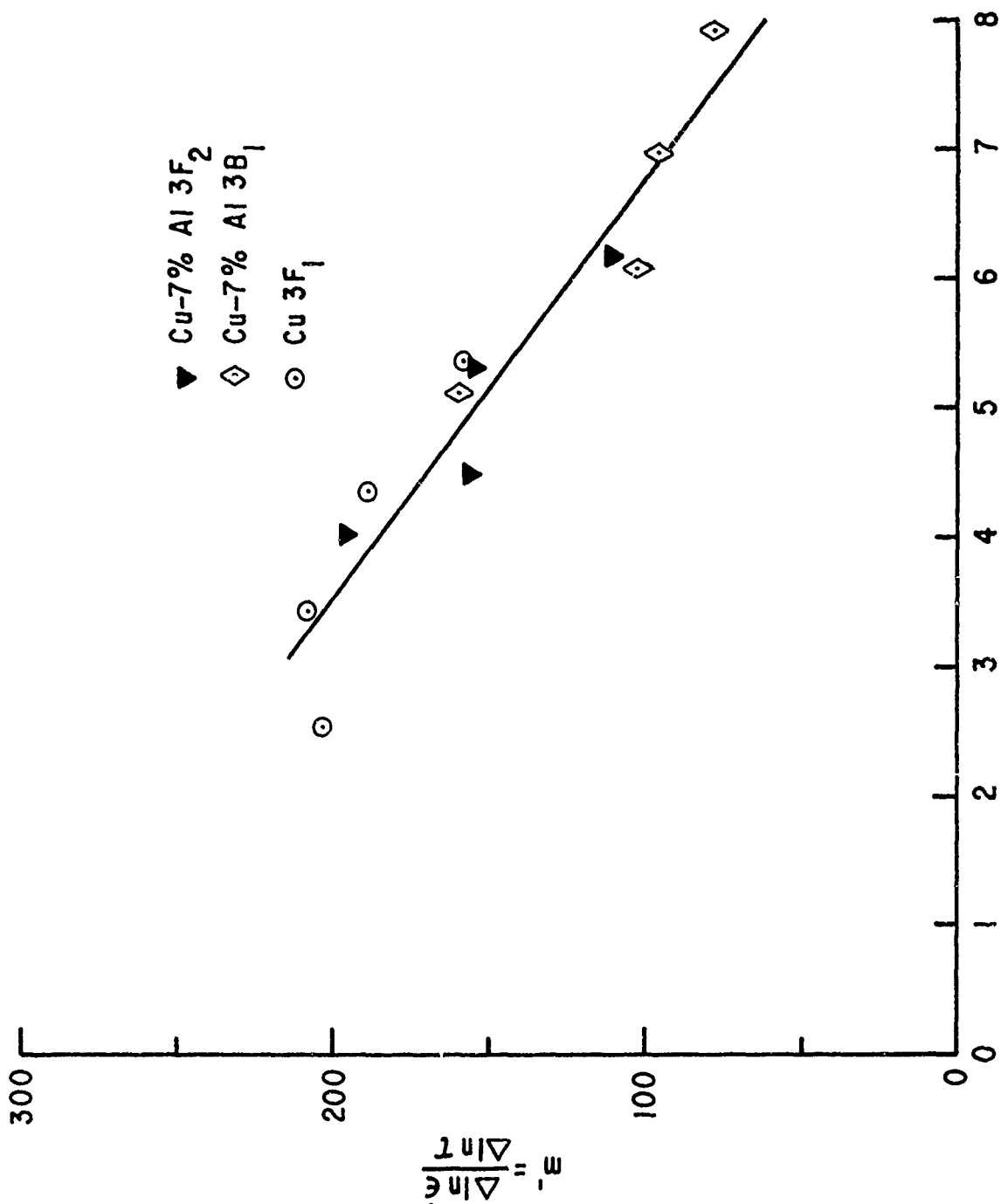

Figure 23. Strain Rate Sensitivity versus Strain for Pure Copper and Two Copper-7 Percent Aluminum Alloys

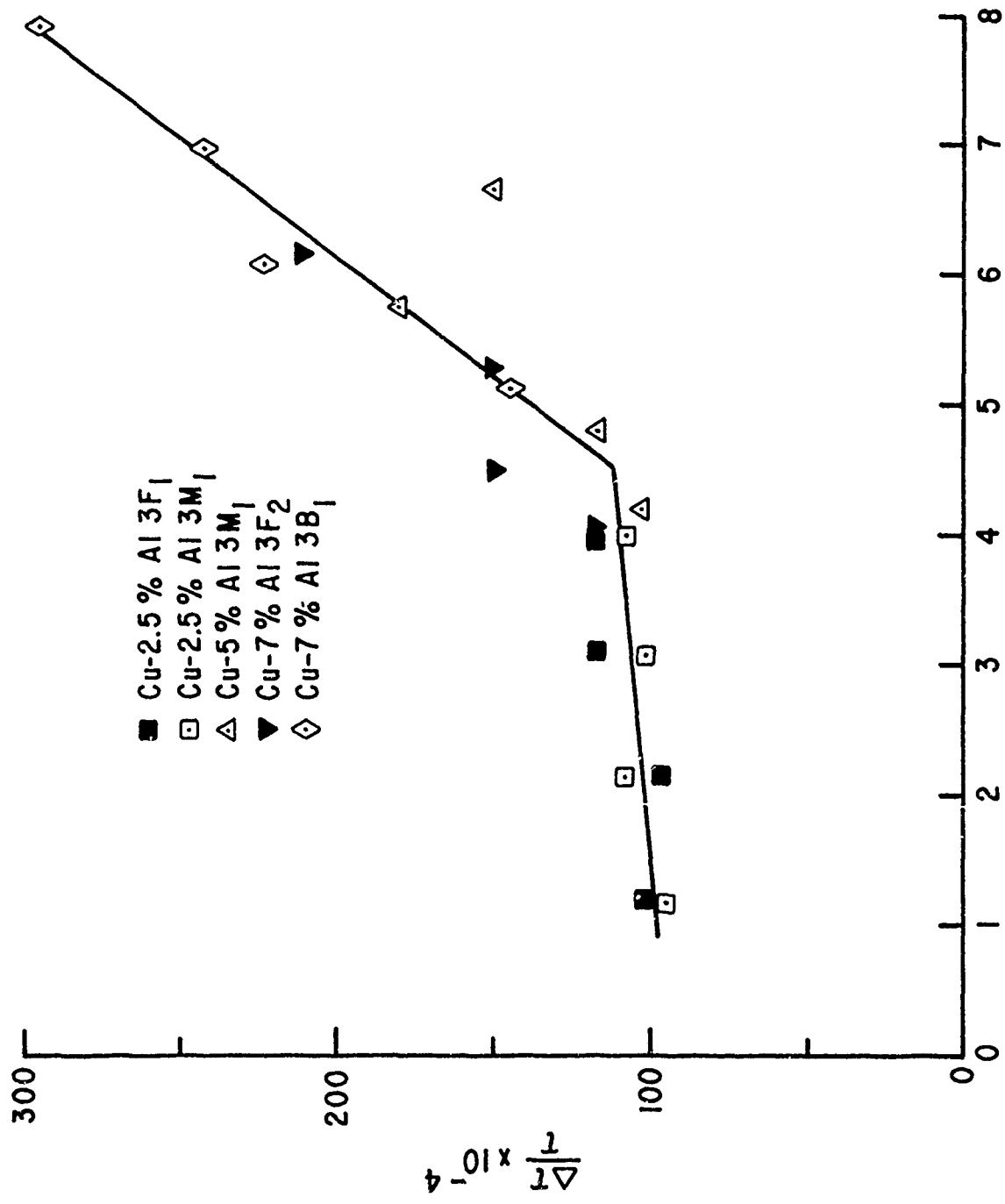

Figure 24. Cottrell-Stokes Parameter versus Strain

SECTION IV

DISCUSSION

All of the transmission electron micrographs clearly indicate that near the front surface, where the intensity of the shock wave is the greatest, plastic deformation was initiated on all of the principal face-centered-cubic slip systems. The attenuation of the shock wave into the metal crystals is accompanied by a decrease in the dislocation and point defect densities. In addition, the plastic deformation is restricted to two and then to only one active slip system as the shock wave propagates to the rear of each of the samples. The dislocation densities are not uniform throughout each slice but are seen to be clustered into high dislocation density areas and areas devoid of these line defects. This effect is especially true of the copper-5 percent aluminum alloy as well as the copper-7 percent aluminum alloy where cell formation is seen (see for example, figure 9). We are encouraged to think that the dislocation densities reported here are realistic and reflect the actual defect density existing at the time of the shock loading for two reasons: (1) the dislocations are pinned in place by the simultaneous production of vacancies and vacancy clusters due to the radiation, and (2) there is a linear relationship between the reported yield stress and the square root of dislocation density shown in figure 17, regardless of the position of the slice below the front surface. For example, on the curve for pure copper, the dislocation density/yield stress relationship is reversed for the point (3F1) and (3F2) and reflects the fact that while the point (3F1) was closest to the incident surface it nevertheless developed a lower dislocation density and consequently displays a lower yield stress. This is also true of the copper-2.5 percent aluminum curve where the reported dislocation density for slice (3B2) is larger than that reported for slice (3B1) (although the former slice is 0.04 inch deeper than the latter slice) and therefore the measured yield stresses appear on that curve in this same order.

The strain rate sensitivity parameter, m', is derived from the following empirical expression of Johnston and Gilman (ref. 4):

$$v = A\tau^{m} \qquad (1)$$

where v refers to the mean dislocation velocity, τ is the resolved shear stress (applied), and A and m are material parameters. In terms of the dislocation density, the rate of strain of a crystal is expressed as

$$\dot{\varepsilon} = b \bar{v} N \tag{2}$$

where b is the Burgers vector and N is the density of the mobile dislocations. The strain rate sensitivity factor, m', derived from differentiating (1) and (2) above, is

$$m' = \frac{\partial \ln \dot{\varepsilon}}{\partial \ln \tau} = \frac{\partial \ln N}{\partial \ln \tau} + \frac{\partial \ln v}{\partial \ln \tau} \tag{3}$$

It is seen from the derivative of equation (1) that m' is related to the change in the mobile dislocation density by

$$m' = m + \frac{\partial \ln N}{\partial \ln \tau} \tag{4}$$

Johnston and Stein (ref. 5) have indicated that m' approaches value of m only at small strains. This is in contradiction to Guard (ref. 6), who pointed out that m' equals m if the second term in equation (4) is negligible. This implies a constancy in the mobile dislocation density as the strain rate is suddenly changed. This assumption does not necessarily occur since the sudden increase in stress accompanying a sudden change in strain rate may unpin dislocations and make them mobile. Consequently, N will not be a constant. Plots of the strain rate sensitivity parameter, m', versus percent strain can therefore show an increase as the strain increases (see, for example, figure 21 of the present work). Johnston and Stein (ref. 5) have extrapolated these curves to 0 percent strain and have shown that the value of m thus determined approaches the value of m determined from their etch-pit velocity measurements.

From equation (3) it is seen that if the rate of change of the log of the velocity with respect to the rate of change of the log of the applied shear stress is constant, then increases in m' reflect increases in the rate of change of the log of N with changes in the log of the applied shear stress. Thornton, Mitchell, and Hirsch (ref. 7) studied the strain rate sensitivity of copper single crystals as a function of the shear stress. The strain rate sensitivity was reported to increase sharply from a value of approximately 100 at the lower

shear stress values and asymptotically approach the value of 225 where the single crystal deformation changed from stage II to the beginning of stage III. At this level the single crystal values of the strain rate sensitivity approached those of polycrystalline copper deformed at room temperature. This experimental determination of the independence of the strain rate sensitivity with deformation at large strains by Thornton et al. (ref. 7) was also found to be true in the present work. For example, see the results for pure copper in figure 18. In this plot all strain rate changes were made from the same strain rate base of 0.01 inch per inch per minute. The average value of the strain rate sensitivity of 180, however, is somewhat lower than the 225 value for m' reported by Thornton et al. In addition, the determination of the strain rate sensitivity factor as a function of the shear stress for copper-2.5 percent aluminum (figure 19) duplicates very closely the previous work of Thornton et al. for copper. The strain rate sensitivity factor for copper-7 percent aluminum is also found to be independent of the state of deformation (figure 20). However, the average value for the (3M2) slice is approximately 100, while the average value for slice (3B2) is near 75. Lower values of the strain rate sensitivity have been reported for copper-5 percent silicon single crystals by Evans (ref. 8) where m' rises from a value of 60 for a shear stress of 2 kg/mm^2 to a value of 180 at a shear stress of 10 kg/mm^2. What is most interesting is that while the strain rate sensitivity for the copper, copper-2.5 percent aluminum, and copper-7 percent aluminum was independent of strain, the strain rate sensitivity for the copper-5 percent aluminum slice (3F2) increased from values near 100 to values near 250 as the strain increased.

Invariance of the value of m' with deformation implies that neither the velocity of dislocations nor the number of mobile dislocations is changing during further straining of the crystal. The data of Thornton et al. (ref. 7) on pure single crystal copper suggests that regions of deformation where m' is independent of the strain occur when the single crystal has entered stage III and is behaving in a manner similar to a polycrystalline material. Based on this subdivision of the single crystal stress strain curve, the strain rate sensitivity curves for the copper, copper-2.5 percent aluminum, and copper-7 percent aluminum would indicate that stage III had been reached almost immediately at the start of their tensile testing. On the other hand, the strain rate sensitivity factor for copper-5 percent aluminum is seen to increase with the strain, indicating that the crystal is still deforming in stage II, the linear work-hardening region.

In the present work the strain rate sensitivity factor was also determined for strain rate changes of one order of magnitude, but here the base from which the strain rate changes were made constantly increased with the deformation. See, for example, figure 15 in which five strain rate changes are reported from 0.001 inch per inch per minute to 10 inches per inch per minute. The strain rate sensitivity determined in this manner, as a function of strain, is shown to decrease linearly for copper-2.5 percent aluminum as well as for copper and copper-7 percent aluminum (figures 22 and 23). The decrease in strain rate sensitivity with strain, for strain rate ratios with different base strain rates, was previously reported by Michalak (ref. 9) for iron single crystals deformed at room temperature.

The Cottrell-Stokes parameter versus deformation was also determined in the present work. Referring to figure 24, it is interesting to note that positive deviations occur for the metals undergoing strain rate changes at higher strain levels while the Cottrell-Stokes law is essentially obeyed for those crystals in which changes in the strain rate occurred at lower deformation.

Since the Cottrell-Stokes parameter compares the ratio of the temperature independent part of the total stress to the temperature dependent part of the flow stress invariance in the parameter implies either that the same dislocation mechanism is responsible for the work hardening process (ref. 8), or that the ratio of short range to long range dislocation barriers remains constant with deformation (ref. 10). Following the treatment of the strain rate sensitivity factor of Evans et al. (ref. 8), which is related to the Cottrell-Stokes parameter, the following relationship between the thermal and athermal components of the flow stress are obtained

$$m' \underset{\varepsilon \to 0}{\to} m^* = \frac{\tau^* V}{KT} \qquad (5)$$

where m^* is the strain rate sensitivity factor when the effective stress, τ^*, is used rather than the applied stress, τ. For small strains m' approaches m^* and is equal to the ratio of mechanical energy to the thermal energy required for activation of a dislocation past a rate-controlling obstacle. Consequently, changes in m^* or m' at constant temperature imply that changes in the internal stress are accompanying the deformation. In the present work, positive deviations from the Cottrell-Stokes relationship are reported for some of the copper and copper alloys, provided that the deformation has proceeded far enough. This

is in agreement with the finding of Mitchell, Foxall, and Hirsch (ref. 11) that copper does not obey the Cottrell-Stokes law, except that in this case deviations were noted at low strain values while in the present work positive deviations occur at large strain values. The temperature independent contribution to the flow stress has been identified by Seeger (ref. 12) to be due to the long range stress fields of dislocations which are produced by dislocation pile-ups. Consequently, in contrast to the cellular dislocation structure developed by the intense shock loading of these samples, the subsequent tensile tests are expected to produce extensive pile-ups behind suitable barriers such as deformation twins. Positive deviation from the Cottrell-Stokes law is then expected for those copper alloys tested at succeedingly increasing strain rates. Evidence of this type of dislocation morphology is presented in figures 25 and 26 from a copper-7 percent aluminum specimen strained 8.4 percent in tension after shock loading. The presence of twins is clearly indicated in both the diffraction pattern and the microphotograph where profuse pile-up of dislocations is shown. The formation of mechanical twins in single crystals of copper-3.6 percent aluminum from stacking fault nuclei has recently been reported by Fujita and Mori (ref. 13). The present work essentially corroborates their findings that (1) twinning occurs after a considerable amount of prior deformation, (2) twins are easily formed near pre-existing stacking faults, and (3) twin formation becomes easier as the tensile axis approaches <111> (the axis used in the present work). Deformation-produced twinning is further implied to occur at the higher strains in the stress strain curves for all of the crystals tested (figures 14 and 15), when an order of magnitude change in the strain rate to 10 inches per inch per minute results in a serrated, Portevin-le Chatelier flow curve.

Figure 25. Copper-7 Percent Aluminum 3B1, Tensile Strained 8.4 Percent after Shock Loading with Defraction Patterns Showing Twin Spots (T) and Streaking (S) Due to Twin Stacking Faults

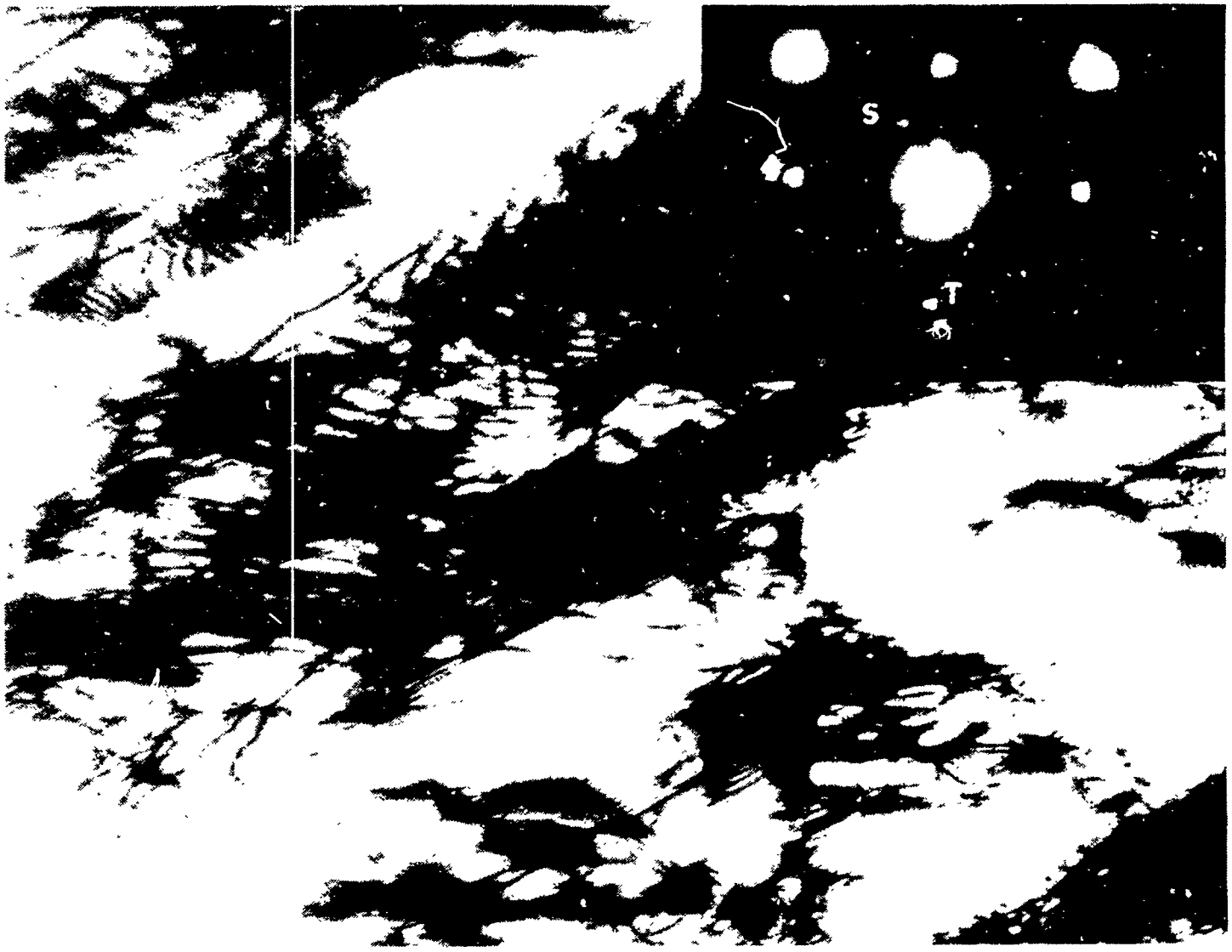

Figure 26. Copper-7 Percent Aluminum 3B1, Tensile Strained 8.4 Percent after Shock Loading with Defraction Patterns Showing Twin Spots (T) and Streaking (S) Due to Thin Stacking Faults

SECTION V

CONCLUSIONS

1. Shock induced plastic deformation is activated on all slip systems of face-centered-cubic metals near the front surface but is confined to two and then to only one slip system near the rear of the samples.

2. Extrinsic stacking faults (twins) are nucleated by 50 kilobars pressure in copper-5 percent aluminum.

3. The yield stress was found to vary with the square root of the dislocation density, N, regardless of the position of the specimen within each sample.

4. The strain rate sensitivity factor, m', was found to be invariant with deformation for some of the copper, copper-2.5 percent aluminum, and copper-7 percent aluminum samples. According to Thornton, Mitchell, and Hirsch, this indicates that the metals are deforming in stage III.

5. The strain rate sensitivity factor, m', decreases with deformation if the same changes (one order of magnitude) in strain rate are made at successively higher base strain rates. Examples were shown for copper, copper-2.5 percent aluminum, and copper-7 percent aluminum.

6. For several of the samples, the strain rate sensitivity factor, m', increases with deformation. Johnston and Stein (ref. 5), Guard (ref. 6), and others have shown that this same relationship holds for LiF and silicon-iron and also indicated that $m' \rightarrow m$ as $\varepsilon \rightarrow 0$. Following Li's suggestion that changes in m' with deformation imply changes in both dislocation density, N, and the internal stress, σ, then an increase in m' means that the athermal part of the flow stress has increased. An increase of the temperature invariant contribution to the flow stress for the 5 percent and 7 percent aluminum alloys was shown to be due to dislocation pile-ups which occur at higher strains. This implies that in those alloys where m' varies with deformation the samples have changed their dislocation morphology from a cellular structure to one of linear arrays and heavy slip bands. Direct evidence that twins act as barriers to these dislocation pile-ups is presented in figures 25 and 26.

REFERENCES

1. Smith, C. S., and Guttman, L., Trans. AIME, 197, 1953, p. 81.
2. Steeds, J. W., Proc. Royal Society A., 292, p. 343, 1966.
3. Hirsch, P. B., Howie, A., Nicholson, R. B., Pashely, D. W., and Whelan, M. J., Electron Microscopy of Thin Crystals, Butterworths, 1965, p. 423.
4. Johnston, W. G., and Gilman, J. J., J. Appl. Phys., 30, 1959, p. 129.
5. Johnston, W. G., and Stein, D. F., Acta Met 11, 1963, p. 317.
6. Guard, R. W., Acta Met. 9, 1961, p. 163.
7. Thornton, P. R., Mitchell, T. E., and Hirsch, P. B., Phil Mag 7, 1962, p. 337.
8. Evans, K. R., Bailey, D. J., and Flanagan, W. F., Phys Stat Sol 22, 1967, p. 607.
9. Michalak, J. T., Acta Met., 13, 1965, p. 213.
10. Wilsdorf, D. K., Trans Aime, 224, 1962, p. 1047.
11. Mitchell, T. E., Foxall, R. A., and Hirsch, P. B., Phil. Mag. 8, 1963, p. 1895.
12. Seeger, A., Dislocations and Mechanical Properties of Crystals, John Wiley and Sons, 1957, p. 243.
13. Fujita, H., and Mori, T., Scripta Met 9, 1975, p. 631.